Nuclear Physics B160 (1979) 151-207

ONE-LOOP CORRECTIONS FOR e^+e^- ANNIHILATION INTO $\mu^+\mu^-$ IN THE WEINBERG MODEL

G. PASSARINO* and M. VELTMAN
Institute for Theoretical Physics, University of Utrecht, Utrecht, The Netherlands

Received 22 March 1979

Analytical expressions for the $e^+e^- \to \mu^+\mu^-$ cross section including all the one-loop radiative corrections in the context of the Weinberg model are presented. The systematic calculation of one-loop diagrams has been carried out using a recently proposed scheme. Numerical results are shown in a region from 40-200 GeV c.m. energy and different values of the scattering angle; they indicate that the percentage corrections are mainly due to soft photons. The only departure from QED-like corrections can be seen in a region where the lowest-order cross section is lowered by weak-e.m. interference. In that region hard photon contributions are relatively prominent and perhaps within experimental possibilities.

1. Introduction

In recent years experiment and theory of weak and e.m. interactions have developed to a point that there is now a general consensus on the validity of the Weinberg model, at least in some effective sense. The principal feature of this model is the renormalizability [1], and one of the fundamental ingredients is the Higgs particle.

In a systematic investigation of the validity of this model one must sooner or later consider the radiative corrections. These radiative corrections, finite by virtue of the renormalizability of the theory, will be an indispensible part of the verification of the theory. Moreover, at some point the Higgs meson will play an essential role in the actual result, and perhaps we may get information on the Higgs meson even without actually producing it. For this reason we have started a systematic calculation of radiative corrections†.

As a first step a scheme must be developed that makes these calculations feasible. In ref. [3] a collection of formulae valid for scalar one-loop diagrams has been given; all other one-loop integrals are algebraically related to these scalar expressions. The method is then simply the following: (i) develop a computer program

* On leave from: Istituto di Fisica Teorica, Universita di Torino, Italy.
† Calculations of radiative corrections in QED on similar processes can be found in refs. [2].

that provides for numerical answers to the one-loop functions given the numerical values of the various parameters (energy, masses etc.), and (ii) write for a given process all diagrams in terms of these one-loop functions. This is the strategy that we have adopted in this paper and in fact the present calculation serves also to demonstrate the feasibility of this procedure.

The case that we concentrate on is the process e^+e^- annihilation into $\mu^+\mu^-$. From an experimental point of view this seems to be the easiest process, and theoretically it is very clear and well-defined. In doing this calculation we are confronted with the usual divergencies of the theory, namely infrared and ultraviolet. The infrared divergencies are treated in the usual way by inclusion of soft bremsstrahlung. In the actual calculations we keep the photon mass small but finite, and in the end we verify that the total result is invariant against variations in the value of this photon mass, at least for small values of that mass. The ultraviolet divergencies are treated by defining quantities δg, δM etc., one for each parameter of the theory, and subsequently fixing each of these quantities by comparison with the data. In the case at hand it turns out that three data points are needed to fix δg, δM and $\delta \sin\theta$, where θ is the weak mixing angle. We emphasize that this fitting is a numerical procedure. In our calculations infinity is represented by a parameter Δ, and the values of the quantities δg etc., will depend on this Δ. But after renormalization the answers must be independent of A, which is a strong test on the internal consistency of the whole calculation.

The results may be summarized as follows. The major part of the radiative corrections are due to soft photons, either real (bremsstrahlung) or virtual. In some sense these corrections are not very interesting since they do not depend on the detailed mechanisms of the process, but rather on the in- and outgoing charges. However, there is a region where the soft photon contribution is relatively small, and in that region hard photon corrections become visible, and are perhaps experimentally accessible. This is before and after the neutral vector boson resonance, i.e., around 75 and 105 GeV. The dependence on the Higgs mass of all corrections at all energies and momenta transfers that we have considered is vanishingly small, and appears to be beyond experimental possibilities.

In carrying through the above program we made the approximation of small lepton masses, and furthermore we have not treated hard bremsstrahlung. In particular hard bremsstrahlung may be very important precisely in the region where the soft photon corrections are small, and in this sense this paper is incomplete. Of course, the hard bremsstrahlung calculation is quite independent of the corrections treated in this paper.

The outline of the paper is as follows. In sect. 2 we describe the model. In sect. 3 the lowest-order cross section is given. In sect. 4 we list the one-loop diagrams which are considered separately and computed in sects. 5-8. Bremsstrahlung is analyzed in sect. 9. Sect. 10 explains the renormalization procedure we have adopted. Conclusions and numerical results are given in sect. 11. In several appendices technical details are given.

2. The model

Within the Weinberg model there is a triplet of vector bosons B^a_μ, a singlet B^0_μ, a complex scalar field K and the lepton families e, ν_e; μ, ν_μ. The physical fields $W^\pm_\mu$, W^0_μ, A_μ are related to B^a_μ, B^0_μ by (2.1)

$$W^\pm_\mu = \sqrt{\tfrac{1}{2}}(B^1_\mu \mp iB^2_\mu), \qquad W^0_\mu = c_\theta B^3_\mu - s_\theta B^0_\mu, \qquad A_\mu = s_\theta B^3_\mu + c_\theta B^0_\mu,$$

where s_θ, c_θ denote the sin and the cos of the weak mixing angle. We also introduce

$$K = \sqrt{\tfrac{1}{2}}\begin{pmatrix} Z + \sqrt{2}F + i\phi^3 \\ -\phi^2 + i\phi^1 \end{pmatrix},$$
$$\phi^3 \equiv \phi^0, \qquad \phi^\pm = \sqrt{\tfrac{1}{2}}(\phi^1 \mp i\phi^2). \tag{2.2}$$

The following conventions are used

$$\psi_\pm = \begin{pmatrix} \nu_\pm \\ \ell_\pm \end{pmatrix}, \qquad \nu_\pm = \tfrac{1}{2}(1 \pm \gamma^5)\nu, \qquad \ell_\pm = \tfrac{1}{2}(1 \pm \gamma^5)\ell.$$

The representation of the symmetry group SU(2)xU(l) is given by the generators

$$T_a = -\tfrac{1}{2}i\tau_a, \qquad T_0 = -\tfrac{1}{2}g_2\tau_0,$$

and

$$t_a = 0, \qquad t_0 = -\tfrac{1}{2}ig_3\begin{pmatrix} 0 & 0 \\ 0 & 1 \end{pmatrix}, \tag{2.3}$$

with for any multiplet arbitrary g_2 and g_3. The τ_i are the Pauli matrices and τ_0 is the identity. The covariant derivatives are

$$D_\mu\psi_+ = (\partial_\mu + gB^i_\mu T_i)\psi_+,$$
$$D_\mu\psi_- = (\partial_\mu + gB^i_\mu t_i)\psi_-,$$
$$D_\mu K = (\partial_\mu - \tfrac{1}{2}igB^a_\mu\tau_a - \tfrac{1}{2}igg_1B^0_\mu\tau_0)K, \qquad (i = 0, 1, 2, 3). \tag{2.4}$$

The coupling constant g_1 determines the mixing angle θ: $g_1 = -s_\theta/c_\theta$. The Lagrangian is taken to be

$$\mathcal{L} = \mathcal{L}_{\mathrm{YM}}(B^a_\mu) + \mathcal{L}_{\mathrm{YM}}(B^0_\mu) - \bar{\psi}_+\not{D}\psi_+ - \bar{e}_-\not{D}e_- - (D_\mu K)^+D^\mu K - \mu K^+K$$
$$-\tfrac{1}{2}\lambda(K^+K)^2. \tag{2.5}$$

Here we have omitted the fermion mass term and lepton-Higgs couplings. The constants g_2 and g_3 are fixed by the conditions that the photon field A_μ is not coupled to the neutrino's and that it has no $\gamma^\mu\gamma^5$ coupling. This gives $g_2 = g_1$ and $g_1 + g_2 = g_3$. The gauge is fixed by adding to the Lagrangian a term $-\frac{1}{2}C^2$ where

$$\mathcal{L}_{\mathrm{g.f.}} = -\tfrac{1}{2}C^2 = -\tfrac{1}{2}(-\partial_\mu B^a_\mu + M\phi^a)^2 - \tfrac{1}{2}(-\partial_\mu B^0_\mu + g_1M\phi^0)^2. \tag{2.6}$$

The ghost fields are X^0, X^a (a = 1,2,3) and the associated ghost Lagrangian together with the Lagrangians (2.5), (2.6) are given in appendix A in terms of the physical fields.

The zero mass of the photon will produce infrared divergences into the radiative corrections to the process, which need to be regularized by giving the photon a small mass λ. To avoid a breakdown of the U(l) gauge invariance we can introduce this λ by means of spontaneous symmetry breakdown. This gives rise to extra vertices proportional to this same λ; however, they can be neglected since the infrared behavior is at most as In λ. In $e^+e^- \to \mu^+\mu^-$ and in all the processes with no external vector lines we neglect systematically the coupling of the Higgs particles to the fermions since they are proportional to the lepton mass. A list of the vertices in the one-loop corrections is given in appendix B.

3. $e^+e^- \to \mu^+\mu^-$ lowest order

The following notations and conventions are used (see fig. 1):

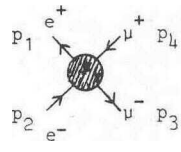

Fig. 1. The process $e^+e^- \to \mu^+\mu^-$.

All the momenta are incoming, and our metric is such that a timelike momentum squared is negative. p_1 = incoming e^+; p_2 = incoming e^-; $-p_3$ = outgoing μ^-; $-p_4$ = outgoing μ^+:

$$p_1^2 = p_2^2 = -m_e^2, \qquad p_3^2 = p_4^2 = -m_\mu^2,$$
$$s = -(p_1+p_2)^2, \qquad t = -(p_1+p_4)^2, \qquad u = -(p_1+p_3)^2,$$
$$u = -s - t + 2(m_e^2 + m_\mu^2). \tag{3.1}$$

Further M, M_0 and m are $W^\pm$, W^0 and Higgs masses. In lowest order (fig. 2) two diagrams contribute to the amplitude for $e^+e^- \to \mu^+\mu^-$:

$$A_0 = (2\pi)^4 i g^2 \left\{ \frac{s_\theta^2}{-s} \bar{u}(-p_3)\gamma^\mu v(-p_4)\bar{v}(p_1)\gamma^\mu u(p_2) \right.$$
$$\left. + \frac{1}{16c_\theta^2}\frac{1}{-s+M_0^2}\bar{u}(-p_3)\gamma^\mu(v_\theta - \gamma^5)v(-p_4)\bar{v}(p_1)\gamma^\mu(v_\theta - \gamma^5)u(p_2) \right\}, \tag{3.2}$$

where $v_\theta = 4s_\theta^2 - 1$. The corresponding lowest-order cross section in the limit of

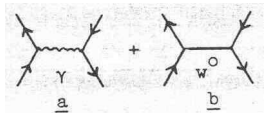

Fig. 2. Lowest-order diagrams for $e^+e^- \to \mu^+\mu^-$.

small lepton mass is:

$$\frac{d\sigma^0}{d(\cos\theta_s)} = \sigma_E^0 + \sigma_W^0 + \sigma_I^0,$$

$$\sigma_E^0 = \frac{g^4}{16\pi} s_\theta^4 \frac{A_E(s,t)}{s} \equiv \frac{g^4}{16\pi} s_\theta^4 \frac{x(s,t)}{s},$$

$$\sigma_W^0 = \frac{g^4}{128\pi} \frac{A_W(s,t)}{(-s+M_0^2)^2}, \qquad \sigma_I^0 = \frac{-g^4}{128\pi} \frac{A_I(s,t)}{s(-s+M_0^2)}, \tag{3.3}$$

where

$$A_W(s,t) = \frac{v_\theta^4}{32c_\theta^4} sx(s,t) + \frac{v_\theta^2}{16c_\theta^4}[2s+4t+sx(s,t)] + \frac{1}{32c_\theta^4} sx(s,t),$$

$$A_I(s,t) = v_\theta^2 \frac{s_\theta^2}{c_\theta^2} sx(s,t) + \frac{s_\theta^2}{c_\theta^2}(s+2t),$$

with

$$x(s,t) = 1 + 2\left(\frac{t}{s} + \frac{t^2}{s^2}\right). \tag{3.4}$$

If E denotes the energy per particle and θ_s the scattering angle, then s and t are given by

$$s = 4E^2, \qquad t = m_e^2 + m_\mu^2 - 2E^2 + 2\sqrt{E^2 - m_e^2}\sqrt{E^2 - m_\mu^2}\cos\theta_s \simeq 2E^2(\cos\theta_s - 1). \tag{3.5}$$

The W^0 exchange diagram changes the structure of pure QED angular distribution with the introduction of terms linear in $\cos\theta_s$. The resulting asymmetry is given by

$$d\sigma^0(\theta_s) - d\sigma^0(\pi - \theta_s) = \frac{g^4}{64\pi} \frac{1}{c_\theta^4} \left(\frac{v_\theta^2}{8} \frac{s}{-s+M_0^2} - s_\theta^2 c_\theta^2\right) \frac{\cos\theta_s}{-s+M_0^2}. \tag{3.6}$$

We have neglected terms proportional to the electron or muon mass.

4. Radiative corrections

The cross section for $e^+e^- \to \mu^+\mu^-$ including one-loop corrections is the sum of various contributions that will be computed in the following sections. We write

$$d\sigma = d\sigma^0 + d\sigma^\Delta + d\sigma^M + d\sigma^v + d\sigma^{WR} + d\sigma^B + d\sigma_s^{BR} + d\sigma^{ren}.$$

$d\sigma^0$ is the lowest-order cross section; $d\sigma^\Delta$ is due to photon and W^0 self-energy diagrams (figs. 3a,b). At the one-loop level also a mixing appears between photon and W^0 (diagrams of figs. 3c,d) and the corresponding contribution is denoted by t $d\sigma^M$. Vertex corrections of fig. 4 contain the diagrams V_1–V_7 of appendix C in each blob and give rise to $d\sigma^V$. Next $d\sigma^{WR}$ takes care óf the external line corrections (fig. 5) where the wave-function renormalization has been computed from diagrams W_1–W_3 of appendix C. The contribution $d\sigma^B$ is due to direct and crossed box diagrams, denoted by B_1–B_9 in appendix C, and $d\sigma_s^{BR}$ is the bremsstrahlung cross section in the soft photon approximation computed from the diagrams BR_1–BR_4 of sect. 9. Finally $d\sigma^{ren}$ contains counterterms arising from renormalization. The algebraic complications due to traces of γ matrices, substitutions of variables, reduction to form factors were treated with the help of the computer program SCHOONSCHIP [5].

5. Self-energy diagrams

In this section we will give the results for various types of self-energy diagrams. We go beyond what is strictly needed for $e^+e^- \to \mu^+\mu^-$; the reason is twofold, namely (i) this part of the calculation will be relevant for many other processes, and (ii) to be sure of our expression we want to test the Ward identities valid for these diagrams.

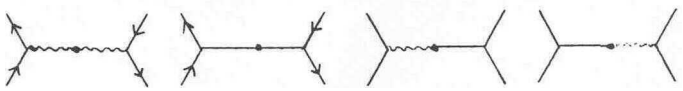

Fig. 3. Diagrams with one-loop corrected propagators and mixing.

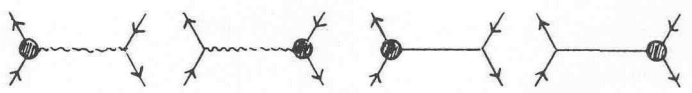

Fig. 4. Vertex diagrams.

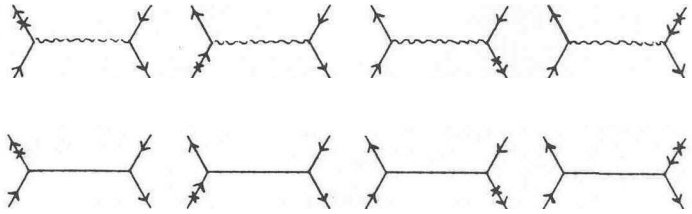

Fig. 5. External line correction.

We will now list the expressions for the various diagrams, and subsequently indicate the Ward identities that they obey.

First there are the vector-vector type self-energy diagrams. The contribution of a graph f is of the form (g = coupling constant):

$$i\pi^2 g^2[A_f\delta_{\mu\nu} + B_f k_\mu k_\nu]. \tag{5.1}$$

The superscripts +, 0, p and 0p indicate contributions relevant to charged W, neutral W, photon and neutral W-photon self-energies respectively. The graphs are classified with respect to the possible internal lines. An internal W-line signifies a vector boson or photon, as the case may be. The functions A, B_0... are defined in the appendices.

Graph S_1. Two W internal lines. Define

$$A_1(k, m_1, m_2) = -[(m_1^2 + m_2^2 - 4k^2)B_0(k, m_1, m_2) - A(m_1) - A(m_2) - 10B_{22}(k, m_1, m_2) - 2(m_1^2 + m_2^2 + \tfrac{1}{3}k^2)],$$

$$B_1(k, m_1, m_2) = -[-10B_{21}(k, m_1, m_2) - 10B_1(k, m_1, m_2) + 2B_0(k, m_1, m_2) + \tfrac{2}{3}].$$

The various contributions are:

$$A_1^+ = c_\theta^2 A_1(k, M_0, M) + s_\theta^2 A_1(k, 0, M),$$

$$B_1^+ = c_\theta^2 B_1(k, M_0, M) + s_\theta^2 B_1(k, 0, M),$$

$$A_1^0 = c_\theta^2 A_1(k, M, M), \qquad B_1^0 = c_\theta^2 B_1(k, M, M),$$

$$A_1^p = s_\theta^2 A_1(k, M, M), \qquad B_1^p = s_\theta^2 B_1(k, M, M),$$

$$A_1^{0p} = c_\theta s_\theta A_1(k, M, M), \qquad B_1^{0p} = c_\theta s_\theta B_1(k, M, M).$$

Graph S_2. Four-point vertex with internal W. The contributions to B_z are zero. Define

$$A_2(m) = -(3A(m^2) + 2m^2).$$

Then (note that $A_2(0) = 0$):

$$A_2^+ = A_2(M) + c_\theta^2 A_2(M_0), \qquad A_2^0 = 2c_\theta^2 A_2(M),$$

$$A_2^p = 2s_\theta^2 A_2(M), \qquad A_2^{0p} = 2s_\theta c_\theta A_2(M).$$

Graph S_3. One W and one ϕ (Higgs ghost) internal line:

$$A_3^+ = \frac{s_\theta^4}{c_\theta^2} M^2 B_0(k, M_0, M) + s_\theta^2 M^2 B_0(k, 0, M),$$

$$A_3^0 = 2\frac{s_\theta^4}{c_\theta^2} M^2 B_0(k, M, M), \qquad A_3^p = 2s_\theta^2 M^2 B_0(k, M, M),$$

$$A_3^{0p} = -2\frac{s_\theta^3}{c_\theta} M^2 B_0(k, M, M).$$

The B_3 contributions are zero.

Graph S_4. One W and one Z (physical Higgs) internal line. No B_4 contribution.

$$A_4^+ = M^2 B_0(k, m, M), \qquad A_4^0 = \frac{M^2}{c_\theta^4} B_0(k, m, M_0),$$

$$A_4^{\mathrm{p}} = 0, \qquad A_4^{0\mathrm{p}} = 0.$$

Graph S_5. One Z and one ϕ (physical and ghost Higgs) internal lines.

$$A_5^+ = B_{22}(k, M, m),$$

$$B_5^+ = \tfrac{1}{4}\{B_0(k, M, m) + 4B_1(k, M, m) + 4B_{21}(k, M, m)\},$$

$$A_5^0 = \frac{1}{c_\theta^2} B_{22}(k, M_0, m),$$

$$B_5^0 = \frac{1}{4c_\theta^2}\{B_0(k, M_0, m) + 4B_1(k, M_0, m) + 4B_{21}(k, M_0, m)\},$$

$$A_5^{\mathrm{p}} = A_5^{0\mathrm{p}} = B_5^{\mathrm{p}} = B_5^{0\mathrm{p}} = 0.$$

Graph S_6. Two ϕ internal lines.

$$A_6^+ = B_{22}(k, M_0, M),$$

$$B_6^+ = \tfrac{1}{4}\{B_0(k, M_0, M) + 4B_1(k, M_0, M) + 4B_{21}(k, M_0, M)\},$$

$$A_6^0 = \frac{(c_\theta^2 - s_\theta^2)^2}{c_\theta^2} B_{22}(k, M, M),$$

$$B_6^0 = \frac{(c_\theta^2 - s_\theta^2)^2}{4c_\theta^2}\{B_0(k, M, M) + 4B_1(k, M, M) + 4B_{21}(k, M, M)\},$$

$$A_6^{\mathrm{p}} = 4s_\theta^2 B_{22}(k, M, M),$$

$$B_6^{\mathrm{p}} = s_\theta^2\{B_0(k, M, M) + 4B_1(k, M, M) + 4B_{21}(k, M, M)\},$$

$$A_6^{0\mathrm{p}} = 2\frac{s_\theta}{c_\theta}(c_\theta^2 - s_\theta^2) B_{22}(k, M, M),$$

$$B_6^{0\mathrm{p}} = \frac{s_\theta}{2c_\theta}(c_\theta^2 - s_\theta^2)\{B_0(k, M, M) + 4B_1(k, M, M) + 4B_{21}(k, M, M)\}.$$

Graph S_7. FP ghost internal lines.

$$A_7^+ = -2c_\theta^2 B_{22}(k, M_0, M) - 2s_\theta^2 B_{22}(k, 0, M),$$

$$B_7^+ = -2c_\theta^2\{B_1(k, M_0, M) + B_{21}(k, M_0, M)\} - 2s_\theta^2\{B_1(k, 0, M) + B_{21}(k, 0, M)\},$$

$$A_7^0 = -2c_\theta^2 B_{22}(k, M, M),$$

$$B_7^0 = -2c_\theta^2\{B_1(k, M, M) + B_{21}(k, M, M)\},$$

$$A_7^{\mathrm{p}} = -2s_\theta^2 B_{22}(k, M, M),$$

$$B_7^{\mathrm{p}} = -2s_\theta^2\{B_1(k,M,M)+B_{21}(k,M,M)\},$$
$$A_7^{0\mathrm{p}} = -2s_\theta c_\theta B_{22}(k,M,M),$$
$$B_7^{0\mathrm{p}} = -2s_\theta c_\theta\{B_1(k,M,M)+B_{21}(k,M,M)\}.$$

Graph S_8. Four-point vertices with Z and ϕ internal lines. No B_8 contribution.

$$A_8^{+} = -\tfrac{1}{4}(A(M_0)+A(m)+2A(M)),$$
$$A_8^{0} = -\frac{1}{4c_\theta^2}(A(m)+A(M_0))+2\left(s_\theta^2-\frac{1}{4c_\theta^2}\right)A(M),$$
$$A_8^{\mathrm{p}} = -2s_\theta^2 A(M), \qquad A_8^{0\mathrm{p}} = \frac{s_\theta}{c_\theta}(s_\theta^2-c_\theta^2)A(M).$$

Also tadpole diagrams are required. They have one external Z-line (physical Higgs), and internally a ϕ, FP ghost, W or Z line. Further there is a tadpole vertex with factor β in the Lagrangian. This β must be adjusted so that the total contribution is zero. The various contributions are:

ϕ $$T_1 = -\alpha M(A(M_0)+2A(M)),$$

FP $$T_2 = MA(M)+\frac{M}{2c_\theta^2}A(M_0),$$

W $$T_3 = -4MA(M)-\frac{2M}{c_\theta^2}A(M_0)-2M^3-\frac{MM_0^2}{c_\theta^2},$$

Z $$T_4 = -3\alpha MA(m),$$

β $$T_5 = -\frac{2M}{g}\beta 16\pi^2.$$

The requirement $\Sigma T_i = 0$ fixes β; note that a factor g^2 must be given to T_1–T_4. We find:

$$\beta = \frac{g}{2M}\frac{1}{16\pi^2}(T_1+T_2+T_3+T_4).$$

Here $\alpha = m^2/4M^2$. This same β must be used for the other β-terms in the Lagrangian, i.e., $-\frac{1}{2}\beta(\phi^2+Z^2)$. This gives rise to the two-line $\phi\phi$ and ZZ vertices with factor $-16\pi^2\beta g$, with β as given above. We define β' by

$$\beta' = -\frac{1}{2M}(T_1+T_2+T_3+T_4),$$

and this factor will occur in the $\phi\phi$ and ZZ vertices. Furthermore Higgs ghost self-energies are needed. There are two types of graphs, namely with two charged ϕ external lines, or two neutral ϕ external lines. Omitting a factor g^2 these contributions will be denoted by H^+ and H^0.

Graph H_1. Two W internal lines.

$$H_1^+ = \frac{4s_\theta^4}{c_\theta^2} M^2 B_0(k, M_0, M) + 4s_\theta^2 M^2 B_0(k, 0, M) - \frac{2s_\theta^4}{c_\theta^2} M^2 - 2s_\theta^2 M^2$$

$$H_1^0 = 0 .$$

Graph H_2- W-ϕ internal lines. Define:

$$H_2(m_1, m_2) = 2A(m_1) - A(m_2) + (m_1^2 - 2m_2^2 + 2k^2) B_0(k, m_1, m_2) .$$

Then

$$H_2^+ = \frac{(c_\theta^2 - s_\theta^2)^2}{4c_\theta^2} H_2(M_0, M) + \tfrac{1}{4} H_2(M, M_0) + s_\theta^2 H_2(0, M) ,$$

$$H_2^0 = \tfrac{1}{2}\{A(M) + (2k^2 - M^2) B_0(k, M, M)\} .$$

Graph H_3. Z-W internal lines. Referring to H_2 defined above we have:

$$H_3^+ = \tfrac{1}{4} H_2(M, m), \qquad H_3^0 = \frac{1}{4c_\theta^2} H_2(M_0, m) .$$

Graph H_4. Two ϕ internal lines. Not existing.

Graph H_5. Z-ϕ internal lines.

$$H_5^+ = 4\alpha^2 M^2 B_0(k, M, m). \qquad H_5^0 = 4\alpha^2 M^2 B_0(k, M_0, m) .$$

Graph H_6. FP ghost.

$$H_6^+ = \frac{c_\theta^2 - s_\theta^2}{2c_\theta^2} M^2 B_0(k, M_0, M) ,$$

$$H_6^0 = \tfrac{1}{2} M^2 B_0(k, M, M) .$$

Graph H_7. Four-point vertex with W-line.

$$H_7^+ = 2\left(s_\theta^2 - \frac{1}{4c_\theta^2}\right)(2A(M_0) + M_0^2) - 2A(M) - M^2 ,$$

$$H_7^0 = -\frac{1}{c_\theta^2}(A(M_0) + \tfrac{1}{2} M_0^2) - 2A(M) - M^2 .$$

Graph H_8. Four-point vertex with Z-line.

$$H_8^+ = -\tfrac{1}{2}\alpha A(m), \qquad H_8^0 = -\tfrac{1}{2}\alpha A(m) .$$

Graph H_9. Four-point with ϕ internal line.

$$H_9^+ = -\tfrac{1}{2}\alpha A(M_0) - 2\alpha A(M) ,$$

$$H_9^0 = -\alpha A(M) - \tfrac{3}{2}\alpha A(M_0) .$$

Graph H_{10}. Two-point vertex with β.

$$H_{10}^{+} = \beta', \qquad H_{10}^{0} = \beta'$$

with β' as defined by the tadpole diagrams, see above. Finally we need the ϕ-W transition diagrams. As internal lines one can have the following pairs: ϕW, ZW, Zϕ, FP and WW. There exist three versions: charged ϕW, neutral ϕW and ϕ-photon external lines. They will be denoted by the superscripts +, 0 and p. A common factor ig^2Mk_μ is omitted.

Graph R_1. ϕ - W internal lines. Denning

$$R_1(m_1, m_2) = B_1(k, m_1, m_2) + 2B_0(k, m_1, m_2),$$

we have

$$R_1^{+} = \frac{s_\theta^2(c_\theta^2 - s_\theta^2)}{2c_\theta^2} R_1(M_0, M) - s_\theta^2 R_1(0, M),$$

$$R_1^{0} = -\frac{s_\theta^2}{c_\theta} R_1(M, M), \qquad R_1^{p} = s_\theta R_1(M, M).$$

Graph R_2. Z- W internal lines. Referring to R_1 as defined above we have

$$R_2^{+} = -\tfrac{1}{2}R_1(M, m), \qquad R_2^{0} = -\frac{1}{2c_\theta^3} R_1(M_0, m), \qquad R_2^{p} = 0.$$

Graph R_3. Z- ϕ internal lines. Define

$$R_3(m_1, m_2) = B_0(k, m_1, m_2) + 2B_1(k, m_1, m_2).$$

We find:

$$R_3^{+} = \alpha R_3(M, m), \qquad R_3^{0} = \frac{\alpha}{c_\theta} R_3(M_0, m), \qquad R_3^{p} = 0.$$

Graph R_4. FP internal lines.

$$R_4^{+} = B_1(k, M_0, M) + \tfrac{1}{2}B_0(k, M_0, M) - c_\theta^2 B_1(k, M_0, M) - s_\theta^2 B_1(k, 0, M),$$

$$R_4^{0} = -c_\theta B_1(k, M, M), \qquad R_4^{p} = -s_\theta B_1(k, M, M).$$

Graph R_5. WW internal lines. Referring to R_3 defined above we have:

$$R_5^{+} = -3s_\theta^2 R_3(M_0, M) + 3s_\theta^2 R_3(0, M),$$

$$R_5^{0} = R_5^{p} = 0.$$

The Ward identities that hold for these expressions are as follows. Let us denote by S_1, S_2, ..., R_5 the contributions of the various diagrams precisely as given in the

above. Then:

$$\sum (k^2 B_i^{\mathrm{p}} + A_i^{\mathrm{p}}) = 0 ,$$

$$\sum (k^2 A_1^0 + k^4 B_i^0) + M_0^2 \sum_i H_i^0 + \frac{2k^2 M^2}{c_\theta} \sum R_i^0 = 0 ,$$

$$\sum (k^2 A_i^+ + k^4 B_i^+) + M^2 \sum H_i^+ + 2k^2 M^2 \sum R_i^+ = 0 ,$$

$$\sum (k^2 A_i^{0\mathrm{p}} + k^4 B_i^{0\mathrm{p}}) + \frac{k^2 M^2}{c_\theta} \sum R_i^{\mathrm{p}} = 0 .$$

In the particular process under consideration we need $\gamma\gamma$, $\mathrm{W}^0\mathrm{W}^0$ and $\mathrm{W}^0\gamma$ diagrams, and of these only the $\delta_{\mu\nu}$ part (because the $k_\mu k_\nu$ part gives only contributions proportional to the lepton mass). In addition then the contribution of lepton pairs must be taken into account. One has for the $\ell - \nu_e$ pair the contribution (m = lepton mass)

$$A_\ell^+ = -2B_{22}(k, 0, m) + \tfrac{1}{2}A(m) - \tfrac{1}{2}(m^2 + k^2)B_0(k, 0, m) ,$$

$$A_\ell^0 = \frac{k^2}{8c_\theta^2}(8B_{21}(k, 0, 0) + 4B_1(k, 0, 0) - 2B_0(k, 0, 0))$$

$$+ \frac{k^2}{16c_\theta^2}\{(4s_\theta^2 - 1)^2 + 1\}\{8B_{21}(k, m, m) + 4B_1(k, m, m)$$

$$- 2B_0(k, m, m)\} - \frac{m^2}{2c_\theta^2}B_0(k, m, m) ,$$

$$A_\ell^{\mathrm{p}} = k^2 s_\theta^2 \{8B_{21}(k, m, m) + 4B_1(k, m, m) - 2B_0(k, m, m)\} ,$$

$$A_\ell^{0\mathrm{p}} = -k^2 \frac{s_\theta}{4c_\theta}(4s_\theta^2 - 1)\{8B_{21}(k, m, m) + 4B_1(k, m, m) - 2B_0(k, m, m)\} .$$

In deriving these expressions we have used some identities among the B-functions, for instance:

$$B_{22}(k, m_1, m_2) = -k^2 B_{21}(k, m_1, m_2) + \tfrac{1}{2}A(m_2) + \tfrac{1}{2}(m_1^2 - m_2^2 - k^2)B_1(k, m_1, m_2) .$$

Such identities are useful from a numerical point of view; the aim is to get rid of the terms $A(m)$. This is particularly important for other contributions involving internal vector bosons. Adding the various contributions we define

$$\Sigma_{\mu\nu}^0(s) = i\pi^2 g^2 [A^0(s)\delta_{\mu\nu} + B^0(s)k_\mu k_\nu] , \qquad s = -k^2 , \tag{5,2}$$

and similar expressions for the photon self-energy $\sum_{\mu\nu}^{\mathrm{p}}(s)$ and the photon $-\mathrm{W}^0$ transition $\sum_{\mu\nu}^{0\mathrm{p}}(s)$. The one-loop corrected propagators are then

$$\bar{\Delta}_{\mu\nu}^{\mathrm{p}} = \frac{1}{(2\pi)^4 i}\frac{\delta_{\mu\nu}}{-s}\left[1 - \frac{g^2}{16\pi^2}\frac{A^{\mathrm{p}}}{s}\right] = \frac{1}{(2\pi)^4 i}\frac{\delta_{\mu\nu}}{-s}(1 + \Delta^{\mathrm{p}}) , \tag{5.3}$$

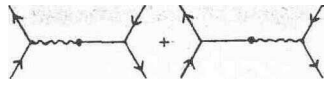

Fig. 6. $\gamma - W^0$ transitions.

$$\bar{\Delta}^0_{\mu\nu} = \frac{1}{(2\pi)^4 i}\frac{\delta_{\mu\nu}}{-s+M_0^2}\left[1+\frac{g^2}{16\pi^2}\frac{A^0(s)-A^0(M_0^2)}{-s+M_0^2}\right] = \frac{1}{(2\pi)^4 i}\frac{\delta_{\mu\nu}}{-s+M_0^2}(1+\Delta^0), \tag{5.4}$$

$$\bar{\Delta}^{0\mathrm{p}}_{\mu\nu} = \bar{\Delta}^{\mathrm{p}0}_{\mu\nu} = \frac{1}{(2\pi)^4 i}\frac{g^2}{16\pi^2}\frac{A^{0\mathrm{p}}(s)}{s(M_0^2-s)}\delta_{\mu\nu}. \tag{5.5}$$

This $\gamma - W^0$ mixing gives a contribution to the g^6 terms of the cross section as given by the diagrams of fig. 6.

$$\begin{aligned}
&\mathrm{d}\sigma^{\mathrm{M}} = \sigma^{\mathrm{M}}_{\mathrm{E}} + \sigma^{\mathrm{M}}_{\mathrm{W}},\\
&\sigma^{\mathrm{M}}_{\mathrm{E}} = -\frac{g^6}{(2\pi)^3}\frac{c_\theta}{64 s_\theta}F_{\mathrm{E}}A^{0\mathrm{p}}, \qquad \sigma^{\mathrm{M}}_{\mathrm{W}} = -\frac{g^6}{(2\pi)^3}\frac{c_\theta}{64 s_\theta}F_{\mathrm{W}}A^{0\mathrm{p}},
\end{aligned} \tag{5.6}$$

$$\begin{aligned}
&F_{\mathrm{E}} = 2\frac{s_\theta^4}{c_\theta^2}v_\theta\frac{x(s,t)}{s(-s+M_0^2)},\\
&F_{\mathrm{W}} = 8\frac{s_\theta^4}{c_\theta^4}\left(\tfrac{3}{4}s_\theta^2 - s_\theta^4\right)\frac{x(s,t)}{(-s+M_0^2)^2}\\
&\quad + \frac{s_\theta^2}{c_\theta^4}\left[(1-6s_\theta^2)\left(\tfrac{1}{2}+\frac{t}{s}\right) + \left(\tfrac{1}{2}-4s_\theta^2\right)\frac{t^2}{s^2}\right]\frac{1}{(-s+M_0^2)^2},
\end{aligned} \tag{5.7}$$

where x is given by (3.4). The A and W^0 self-energies give a cross section

$$\mathrm{d}\sigma^{\Delta} = +\Delta^{\mathrm{p}}(2\sigma^0_{\mathrm{E}} + \sigma^0_{\mathrm{I}}) + \Delta^0(2\sigma^0_{\mathrm{W}} + \sigma^0_{\mathrm{I}}), \tag{5.8}$$

where Δ^{p} and Δ^0 are defined by eqs. (5.3) and (5.4) and σ^0_{E}, σ^0_{I} and σ^0_{W} by eq. (3.3).

6. Fermion wave-function renormalization

The three diagrams contributing to the e, μ wave-function renormalization (W_1-W_3) are obtained as special cases from the expression

$$\begin{aligned}
\Sigma(p^2, m_1, m_2; \lambda_1, \lambda_2) &= g^2\int \mathrm{d}^n q \frac{1}{(q^2+m_1^2)((q+p)^2+m_2^2)}\gamma^\mu(\lambda_1+\lambda_2\gamma^5)\\
&\times(i\not{q}+m_1)\gamma^\mu(\lambda_1+\lambda_2\gamma^5).
\end{aligned} \tag{6.1}$$

Since we are dealing with divergent integrals some care is necessary in performing manipulations with γ-matrices. The result is (see appendix D for the meaning of the *B*-functions)

$$\Sigma(p^2, m_1, m_2; \lambda_1, \lambda_2) = -2i\pi^2 g^2 (f_v^+ - g_A\gamma^5)\left(1+\frac{n-4}{2}\right)B_1(p^2, m_1, m_2)i\not{p}$$
$$+4i\pi^2 g^2 f_v^-\left(1+\frac{n-4}{4}\right)B_0(p^2, m_1, m_2)m_1\,, \tag{6.2}$$

where $f_v^\pm = \lambda_1^2 \pm \lambda_2^2$ and $g_A = 2\lambda_1\lambda_2$. Now B_0 and BI contain the divergent parts $+\Delta$ and $-\frac{1}{2}\Delta$ respectively. With $\Delta = -2/n-4$ we have:

$$\Sigma(p^2, m_1, m_2; \lambda_1, \lambda_2) = -2i\pi^2 g^2 (f_v^+ - g_A\gamma^5)[B_1(p^2, m_1, m_2)+\tfrac{1}{2}]i\not{p}$$
$$+4i\pi^2 g^2 f_v^-[B_0(p^2, m_1, m_2)-\tfrac{1}{2}]m_1\,. \tag{6.3}$$

The electron self-energy is then:

$$\Sigma_e(p^2) = -s_\theta^2\Sigma_e(p^2, m_e, \lambda; 1, 0) - \frac{1}{16c_\theta^2}\Sigma_e(p^2, m_e, M_0; v_\theta, -1)$$
$$-\tfrac{1}{8}\Sigma_e(p^2, 0, M; 1, 1)\,. \tag{6.4}$$

Wave-function renormalization is achieved when we expand $\Sigma(p^2)$

$$\Sigma(p^2) = \Sigma(m_e^2) + \Sigma_{WF}(i\not{p}+m_e) + \Sigma_{rest}(p^2)\,.$$

Further we write:

$$\Sigma_{WF} = i\pi^2 g^2 (W^V + W^A\gamma^5)\,. \tag{6.5}$$

The one-loop corrected electron wave functions are 7):

incoming particle	$\left[1+\frac{g^2}{32\pi^2}(W^V - W^A\gamma^5)\right]u$	$\xrightarrow[p_2]{}$
incoming antiparticle	$\bar{v}\left[1+\frac{g^2}{32\pi^2}(W^V + W^A\gamma^5)\right]$	$\xleftarrow[p_1]{}$
outgoing antiparticle	$\left[1+\frac{g^2}{32\pi^2}(W^V - W^A\gamma^5)\right]v$	$\xleftarrow[p_4]{}$
outgoing particle	$\bar{u}\left[1+\frac{g^2}{32\pi^2}(W^V + W^A\gamma^5)\right]$	$\xrightarrow[p_3]{}$

Fig. 7.

The computation of W^V, W^A requires some additonal work; from (6.5)

$$\Sigma_{WF} = \frac{\partial}{\partial i\not{p}}\Sigma(p^2)|_{i\not{p}=-m_e} = -2i\not{p}\frac{\partial}{\partial p^2}\Sigma(p^2)|_{p^2=-m_e^2}\,. \tag{6.6}$$

We have to compute derivatives of B_0 and B_1 which will be denoted by

$$B_{0p}(-m_e^2, m_1, m_2) = -\frac{\partial}{\partial p^2} B_0(p^2, m_1, m_2)|_{p^2=-m_e^2}, \tag{6.7}$$

and similarly for B_1. From this formula and (6.4) we get for the electron

$$\begin{aligned} W_e^V &= 2s_\theta^2[B_1(-m_e^2, m_e, \lambda) + 2m_e^2 B_{1p}(-m_e^2, m_e, \lambda) + \tfrac{1}{2}], \\ &\quad + 8s_\theta^2 m_e^2 B_{0p}(-m_e^2, m_e, \lambda) \\ &\quad + \frac{v_\theta^2 + 1}{8c_\theta^2}[B_1(-m_e^2, m_e, M_0) + \tfrac{1}{2}] + \tfrac{1}{2}[B_1(-m_e^2, 0, M) + \tfrac{1}{2}], \\ W_e^A &= \frac{v_\theta}{4c_\theta^2}[B_1(-m_e^2, m_e, M_0) + \tfrac{1}{2}] - \tfrac{1}{2}[B_1(-m_e^2, 0, M) + \tfrac{1}{2}]. \end{aligned} \tag{6.8}$$

In eq. (6.8) we have neglected the electron mass where possible. The B_{0p}, B_{1p} functions of QED are infrared divergent and the infrared divergent parts are:

$$\begin{aligned} B_{0p}(-m_e^2, m_e, \lambda) &\sim +\frac{1}{2m_e^2}\left(\ln\frac{m_e^2}{\lambda^2} - 2\right), \\ B_{1p}(-m_e^2, m_e, \lambda) &\sim -\frac{1}{2m_e^2}\left(\ln\frac{m_e^2}{\lambda^2} - 3\right). \end{aligned} \tag{6.9}$$

The infrared-divergent behavior of the wave-function corrections is contained in the self-energy diagram W_1

$$A_{1R}^{WR} = \frac{g^2}{16\pi^2}(W_\mu^V + W_e^V)_{IR} A_0. \tag{6.10}$$

From (6.8), (6.9)

$$\begin{aligned} (W_e^V)_{IR} &= 4s_\theta^2 m_e^2 [B_{1p}(-m_e^2, m_e, \lambda) + 2B_{0p}(-m_e^2, m_e, \lambda)]_{IR} \\ &= 2s_\theta^2 \ln\frac{m_e^2}{\lambda^2}. \end{aligned} \tag{6.12}$$

Thus

$$d\sigma_{IR}^{WR} = \frac{g^2}{16\pi^2} 4s_\theta^2 \left(\ln\frac{m_e^2}{\lambda^2} + \ln\frac{m_\mu^2}{\lambda^2}\right) d\sigma^0. \tag{6.13}$$

To obtain a formula for the cross section we define

$$Z^V = \tfrac{1}{2}[W_e^V + W_\mu^V], \qquad Z^A = \tfrac{1}{2}[W_e^A + W_\mu^A]. \tag{6.14}$$

With this notation we find:

$$d\sigma^{WR} = \frac{g^6}{(2\pi)^3}\frac{1}{256}(\sigma_E^{WR} + \sigma_W^{WR}),$$

$$\sigma_E^{WR} = 32 s_\theta^4 \frac{x(s,t)}{s} Z^v + \frac{y_1(s,t)}{-s+M_0^2} Z^A + \frac{y_2(s,t)}{-s+M_0^2} Z^v,$$

$$\sigma_W^{WR} = \frac{y_1(s,t)}{-s+M_0^2} Z^A + \frac{y_2(s,t)}{-s+M_0^2} Z^v + \frac{z_1(s_\theta)}{c_\theta^4}\left[s x(s,t) - \frac{t^2}{2}\right]\frac{Z^A}{(-s+M_0^2)^2}$$

$$+ \left[\frac{z_2(s_\theta)}{c_\theta^4} s x(s,t) - \frac{z_3(s_\theta)}{c_\theta^4}\frac{t^2}{s}\right]\frac{Z^v}{(-s+M_0^2)^2}, \tag{6.15}$$

where

$$y_1(s,t) = -4\frac{v_\theta}{c_\theta^2} s_\theta^2 \left[x(s,t) - \frac{t^2}{s^2}\right],$$

$$y_2(s,t) = -4\frac{s_\theta^2}{c_\theta^2}(8 s_\theta^4 - v_\theta) x(s,t) + 4\frac{s_\theta^2}{c_\theta^2}\frac{t_\theta^2}{s^2}; \tag{6.16}$$

$$z_1(s_\theta) = -1 + 8 s_\theta^2 - 24 s_\theta^4 + 32 s_\theta^6,$$

$$z_2(s_\theta) = -y_1(s_\theta) + 32 s_\theta^8,$$

$$z_3(s_\theta) = 1 - 8 s_\theta^2 + 16 s_\theta^4, \tag{6.17}$$

and $x(s, t)$ is given by eq. (3.4).

7. Vertex corrections

The most general fermion-fermion-vector coupling (fig. 8) can be reduced to a combination of six form factors.

$$T^\mu = (2\pi)^4 ig[F_v\gamma^\mu + G_A\gamma^\mu\gamma^5 + F_M\sigma^{\mu\nu}p_{5\nu} + F_s p_5^\mu + G_p\gamma^5 p_5^\mu.$$
$$+ G_E\gamma^5(p_1 - p_2)^\mu], \qquad p_5 = p_1 + p_2. \tag{7.1}$$

In the limit of small lepton mass only F_v and G_A contribute and they can be computed starting from the scalar 3-point function C_0 in the same way as we did for self-energies, see appendix E. We may wonder if the small mass limit is always

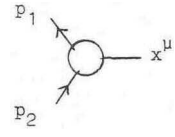

Fig. 8. 3-point vertex.

correct and for this reason we must look at the possible presence of poles in m_e^2. By counting the number of propagators in the 3-point function that can become singular at some point in q space we note that only e.m. corrections can produce such a pole if $p_5^2 = 0$. At this point we must analyze the infrared behavior of the vertex corrections V_1 and V_4 [4]; with our conventions (see appendix E) the virtual photon has momentum $q + p_1$ and the singularity arises from the three poles of the integrand in $q = -p_1$. The coefficient of In λ^2 is obtained by putting everywhere in the numerator $q_\mu = -p_{1\mu}$ and computing the singular part of C_0

$$[C_0, C_\mu, C_{\mu\nu}]_{\mathrm{IR}} = [1, -p_{1\mu}, p_{1\mu}p_{1\nu}] \times \int_{\mathrm{IR}} \mathrm{d}^n q \frac{1}{(q^2+m_e^2)((q+p_1)^2+\lambda^2)((q+p_5)^2+m_e^2)}.$$

Applying the propagator identity of ref. [3] we get

$$\int \mathrm{d}^n q \frac{1}{(q^2+m_e^2)((q+p_1)^2+\lambda^2)((q+p_5)^2+m_e^2)} = \sum_{i=1}^{2} \alpha_i \int \mathrm{d}^n q \frac{1}{(q^2+m_e^2)((q+l)^2+M^2)((q+l+k_i)^2+m_i^2)},$$

where

$$\begin{aligned} &l = p_1 + \alpha p_2, \qquad M^2 = \alpha(1-\alpha)p_2^2 + \alpha m_e^2 + (1-\alpha)\lambda^2 = \alpha^2 m_e^2 + (1-\alpha)\lambda^2, \\ &i = 1, \qquad \alpha_i = 1-\alpha, \qquad k_i = (1-\alpha)p_2, \qquad m_i = m_e, \\ &i = 2, \qquad \alpha_i = \alpha, \qquad k_i = -\alpha p_2, \qquad m_i = \lambda, \end{aligned} \tag{7.2}$$

a in (7.2) is chosen such that $l^2 = 0$; since p_1 and p_2 are time-like α is real.

$$\alpha = \frac{-p_1p_2 \pm \sqrt{(p_1p_2)^2 - p_1^2p_2^2}}{p_2^2} = 1 - \frac{s}{2m_e^2} \mp \frac{s}{2m_e^2}\sqrt{1-4\frac{m_e^2}{s}}. \tag{7,3}$$

We are only interested in the infrared divergent part of (7.2) which is given by:

$$\alpha \int \mathrm{d}^n q \frac{1}{(q^2+m_e^2)((q+l)^2+M^2)((q+p_1)^2+\lambda^2)} = \alpha \int_0^1 \mathrm{d}x \int_0^1 \mathrm{d}y \frac{y}{(Ax+m_e^2)y^2 + (Bx-\lambda^2)y + \lambda^2}, \tag{7.4}$$

where

$$A = 2(\alpha-1)m_e^2 - \alpha s, \qquad B = (1-\alpha)\lambda^2.$$

In deriving (7.4) we have used the equations $(\alpha-1)^2 m_e^2 + \alpha s = 0$ equivalent to $l^2 = 0$; the infrared divergent part of (7.2) is then

$$(C_0)_{IR} = -\tfrac{1}{2}\frac{\alpha}{2(\alpha-1)m_e^2 - \alpha s}\ln\frac{(2\alpha-1)m_e^2 - \alpha s}{m_e^2}\ln\lambda^2$$

$$= -\tfrac{1}{2}\frac{\alpha}{(\alpha^2-1)m_e^2}\ln\alpha^2\ln\lambda^2 \equiv -\tfrac{1}{2}\tau(s, m_e, m_e)\ln\lambda^2 . \tag{7.5}$$

In the general case we get

$$\int_{IR} d^n q \frac{1}{(q^2+m_i^2)((q+p_i)^2+\lambda^2)((q+p_i+p_j)^2+m_j^2)}$$

$$= -\tfrac{1}{2}\frac{\alpha}{\alpha^2 m_j^2 - m_i^2}\ln\left(\frac{m_j^2}{m_i^2}\alpha^2\right)\ln\lambda^2 \equiv -\tfrac{1}{2}\tau(s_{ij}, m_i, m_j)\ln\lambda^2 , \tag{7.6}$$

where $p_{i,j}^2 = -m_{i,j}^2$ and $s_{ij} = -(p_i+p_j)^2$; α is given by

$$\alpha = \frac{-p_i p_j \pm \sqrt{(p_i p_j)^2 - p_i^2 p_j^2}}{p_j^2} . \tag{7.7}$$

The next step will be to show factorization of the infrared divergencies of diagrams 9a-d.

$$A_{IR}^{v} = -(2\pi)^4 i g^2 \frac{g^2}{16\pi^2}\Big[(V^e + V^\mu)\frac{s_\theta^4}{-s}\bar{u}\gamma^\mu v\bar{v}\gamma^\mu u$$

$$+(V^e + V^\mu)\frac{s_\theta^2}{16c_\theta^2(-s+M_0^2)}\bar{u}\gamma^\mu(v_\theta - \gamma^5)v\bar{v}\gamma^\mu(v_\theta - \gamma^5)u\Big]_{IR} . \tag{7.8}$$

In this equation A_{IR}^{v} **is** the infrared divergent part of the one-loop amplitude for vertex corrections. The quantities V are defined in eq. (E.5), appendix E. Comparing eq. (7.8) with the expression for the lowest-order amplitude eq. (3.2) we see:

$$A_{IR}^{v} = -\frac{g^2}{16\pi^2}s_\theta^2(V^e + V^\mu)_{IR}A_0 .$$

Using the results given above:

$$(V^e + V^\mu)_{IR} = -s\Big[\tau(s, m_e, m_e)\ln\frac{m_e^2}{\lambda^2} + \tau(s, m_\mu, m_\mu)\ln\frac{m_\mu^2}{\lambda^2}\Big], \tag{7.9}$$

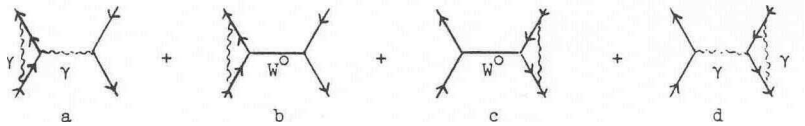

Fig. 9. IR divergent vertex corrections.

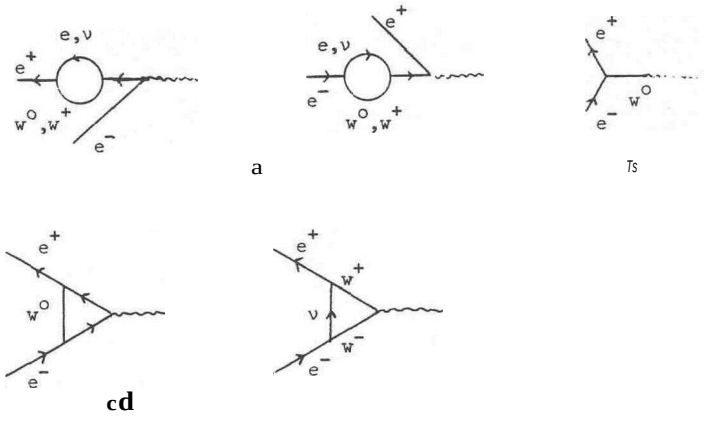

Fig. 10. Vertices contributing to the axial coupling of the photon.

$$d\sigma^{\nu}_{IR} = \frac{g^2}{16\pi^2} s_\theta^2 2s \left[\tau(s, m_e, m_e) \ln \frac{m_e^2}{\lambda^2} + \tau(s, m_\mu, m_\mu) \ln \frac{m_\mu^2}{\lambda^2} \right] d\sigma^0 . \tag{7.10}$$

We now want to check that the fundamental properties built into the Lagrangian are not changed by radiative corrections. No ultraviolet divergence proportional to $\gamma^\mu\gamma^5$ has to be present in the coupling γe^+e^-;this effect could arise from diagrams 10a–d. The total contribution is $i\pi^2 g^3 \gamma^\mu (V + A\gamma^5)$ and (see appendix E for the meaning of the symbols)

$$(A)_a = s_\theta \left\{ -\frac{v_\theta}{4c_\theta^2} [B_1(-m_e^2, m_e, M_0) + \tfrac{1}{2}] + \tfrac{1}{2}[B_1(-m_e^2, 0, M) + \tfrac{1}{2}] \right\},$$

$$(A)_b = \frac{1}{4c_\theta} \frac{\Sigma^{0p}(0)}{M_0^2},$$

$$(A)_c = -\frac{s_\theta}{4c_\theta^2} v_\theta [2C_{24}(0, m_e, M_0, m_e) - 1],$$

$$(A)_d = \tfrac{1}{2} s_\theta [6C_{24}(0, M, 0, M) - 1].$$

The first 0 in the argument of C_{24} represents three external momenta squared. We now consider the pole part in $n-4$:

$$(A)_a = \left(\frac{s_\theta}{4c_\theta^2} v_\theta - \tfrac{1}{2} s_\theta \right) \tfrac{1}{2} \dot{\Delta}, \qquad (A)_b = -\tfrac{1}{2} s_\theta \Delta, \qquad \Delta = -\frac{2}{n-4} + \frac{\delta}{\pi^2},$$

$$(A)_c = -\frac{s_\theta}{8c_\theta^2} \Delta, \qquad (A)_d = \tfrac{3}{4} s_\theta \Delta, \tag{7.12}$$

and the residue of the pole in $n-4$ for the coefficient of $\gamma^\mu\gamma^5$ is zero. For the finite part computed in $s = 0$ we use the following expressions for B_1 and C_{24} in the small lepton mass limit

$$B_0(0, M, M) = -\ln M^2 ,$$
$$B_1(0, 0, M) = \tfrac{1}{2}(\ln M^2 - \tfrac{1}{2}) ,$$
$$C_{24}(0, 0, M_0, 0) = -\tfrac{1}{4}(\ln M_0^2 - \tfrac{3}{2}) ,$$
$$C_{24}(0, M, 0, M) = -\tfrac{1}{4}(\ln M^2 - \tfrac{1}{2}) , \qquad (7.13)$$

which together with (5.10) gives $A = 0$. Thus in the low-energy region there is no parity violation for the e.m. current, as required. Another effect is the $\gamma(\bar{\nu}\nu)$ coupling: the diagrams contributing are given in fig. 11a–c. The $W^0 - \gamma$ transition, diagram 11a, gives

$$i\pi^2 g^3 \bar{u}\gamma^\mu(1+\gamma^5)u \frac{i}{4c_\theta}\frac{\Sigma^{0p}(0)}{M_0^2} = i\pi^2 g^3 \bar{u}\gamma^\mu(1+\gamma^5)u\tfrac{1}{2}is_\theta(-\Delta + \ln M^2) \qquad (7.14)$$

with Δ as before (eq. (7.12)). The vertex diagram 11b gives

$$-i\pi^2 g^3 \bar{u}\gamma^\mu(1+\gamma^5)uis_\theta[C_{24}(0, m_e, M, m_e) - \tfrac{1}{2}] ,$$

and 11c

$$i\pi^2 g^3 \bar{u}\gamma^\mu(1+\gamma^5)u3is_\theta[C_{24}(0, M, 0, M) - \tfrac{1}{6}] . \qquad (7.15)$$

The coefficient of $i\pi^2 g^3 \bar{u}\gamma^\mu(1+\gamma^5)u$ is then

$$-is_\theta\Delta(\tfrac{1}{2} + \tfrac{1}{4} - \tfrac{3}{4}) + is_\theta[\tfrac{1}{2}\ln M^2 + \tfrac{1}{4}(\ln M^2 - \tfrac{3}{2}) + \tfrac{1}{2} - \tfrac{3}{4}(\ln M^2 - \tfrac{1}{2}) - \tfrac{1}{2}] = 0 .$$

In deriving this result we used eq. (7.13) and neglected the lepton masses. Thus there is no ultraviolet divergence contained in the $\gamma(\bar{\nu}\nu)$ coupling and moreover the charge of the neutrino remains zero.

Here we wish to make some comments on these results. In the first instance infinities occurring in these photon couplings (i.e., the $\gamma^\mu\gamma^5$ coupling to electrons or muons, and the coupling to neutrinos) could be renormalized away into the coupling constants g_2 and g_3. However, these constants are not free; if we want to generate the lepton mass with the help of the Higgs system then we must have $g_3 = g_1 + g_2$, and in fact there is a Ward identity assuring this relation. Furthermore

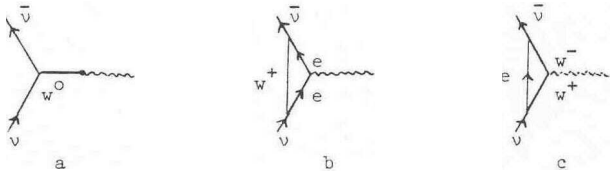

Fig. 11. $\gamma(\bar{\nu}\nu)$ coupling.

there is a Ward identity that assures the vanishing of the neutrino charge, and the above results can therefore be understood as consequences of the symmetry of the theory. We learn from this that g_2 and g_3 need no separate renormalization.

The contributions from vertex corrections to the cross section is the sum of the interference with the lowest order γ and W^0 exchange diagrams figs. 2a,b:

$$d\sigma^{\mathrm{v}} = \frac{g^6}{(2\pi)^3}\frac{1}{256}\sum_{i=1}^{7}[\sigma_{\mathrm{E}}(V_i)+\sigma_{\mathrm{W}}(V_i)]\,. \tag{7.16}$$

The total contribution is made up from a V_i correction into the left and the right vertex.

For i = l, 2,4, 5, 6 we find:

$$\sigma_{\mathrm{E}}(V_i) = F_{\mathrm{E}}(V_i)\sum_{\mathrm{e},\mu}\left[C_{11}+C_{23}-\frac{2}{s}(C_{24}-\tfrac{1}{2})\right]. \tag{7.17}$$

F is a. function of s, t and θ given by

$$F_E(V_1) = -32s_\theta^6 x(s,t)\,,$$

$$F_{\mathrm{E}}(V_2) = -8\frac{s_\theta^4}{c_\theta^2}(4s_\theta^4-\tfrac{1}{2}v_\theta)x(s,t)\,,$$

$$F_{\mathrm{E}}(V_4) = 4\frac{s_\theta^4}{c_\theta^2}(8s_\theta^4-v_\theta)\frac{s}{-s+M_0^2}x(s,t)-4\frac{s_\theta^4}{c_\theta^2}\frac{t^2}{s(-s+M_0^2)}\,,$$

$$F_{\mathrm{E}}(V_5) = 4s_\theta^2\frac{A_W(s,t)}{-s+M_0^2}+2\frac{s_\theta^4}{c_\theta^4}(2s_\theta^2-1)\frac{t^2}{s(-s+M_0^2)}\,,$$

$$F_{\mathrm{E}}(V_6) = 2\frac{s_\theta^2}{c_\theta^2}(2s_\theta^2-1)\frac{s}{-s+M_0^2}x(s,t)+2\frac{s_\theta^2}{c_\theta^2}\frac{t^2}{s(-s+M_0^2)}\,, \tag{7.18}$$

where A_{W}, $x(s,t)$ and v_θ are given in sect. 3. Eq. (7.17) holds also for $\sigma_{\mathrm{W}}(V_i)$ with F_{W} given by

$$F_{\mathrm{W}}(V_1) = 4\frac{s_\theta^4}{c_\theta^2}(8s_\theta^4-v_\theta)\frac{s}{-s+M_0^2}x(s,t)-4\frac{s_\theta^4}{c_\theta^2}\frac{t^2}{s(-s+M_0^2)}\,,$$

$$F_{\mathrm{W}}(V_2) = 4s_\theta^2\frac{A_{\mathrm{W}}(s,t)}{-s+M_0^2}+2\frac{s_\theta^4}{c_\theta^4}(2s_\theta^2-1)\frac{t^2}{s(-s+M_0^2)}\,,$$

$$F_{\mathrm{W}}(V_4) = -4s_\theta^2\frac{s}{(-s+M_0^2)^2}A_{\mathrm{W}}(s,t)\,,$$

$$F_{\mathrm{W}}(V_5) = \frac{1}{c_\theta^6}(-32s_\theta^{12}+48s_\theta^{10}-60s_\theta^8+40s_\theta^6-15s_\theta^4+3s_\theta^2-\tfrac{1}{4})\frac{s^2}{(-s+M_0^2)^2}x(s,t)$$
$$+\frac{1}{c_\theta^6}(32s_\theta^8-32s_\theta^6+14s_\theta^4-3s_\theta^2+\tfrac{1}{4})\frac{t^2}{(-s+M_0^2)^2}\,,$$

$$F_W(V_6) = -\frac{4s_\theta^6 - 6s_\theta^4 + 3s_\theta^2 - \frac{1}{2}}{c_\theta^4}\frac{s^2}{(-s+M_0^2)^2}x(s,t) - \frac{4s_\theta^4 - 3s_\theta^2 + \frac{1}{2}}{c_\theta^4}\frac{t^2}{(-s+M_0^2)^2}. \tag{7.19}$$

For $i = 3, 7$ we can write a formula similar to (7.17):

$$\sigma_{E,W}(V_i) = F_{E,W}(V_i)\sum_{e,\mu}\left[C_0 + C_{11} + C_{23} - \frac{6}{s}(C_{24} - \tfrac{1}{6})\right], \tag{7.20}$$

and

$$F_E(V_3) = 8s_\theta^4 x(s,t),$$

$$F_E(V_7) = 4s_\theta^2(2s_\theta^2 - 1)\frac{s}{-s+M_0^2}x(s,t) + 4s_\theta^2\frac{t^2}{s(-s+M_0^2)},$$

$$F_W(V_3) = -2\frac{s_\theta^2}{c_\theta^2}(4s_\theta^4 - v_\theta)\frac{s}{-s+M_0^2}x(s,t) + 2\frac{s_\theta^2}{c_\theta^2}(1-2s_\theta^2)\frac{t^2}{s(-s+M_0^2)},$$

$$F_W(V_7) = \frac{2}{c_\theta^2}(-4s_\theta^6 + 6s_\theta^4 - 3s_\theta^2 + \tfrac{1}{2})\frac{s^2}{(-s+M_0^2)^2}x(s,t)$$

$$-\frac{2}{c_\theta^2}(4s_\theta^4 - 3s_\theta^2 + \tfrac{1}{2})\frac{t^2}{(-s+M_0^2)^2}.$$

8. Box diagrams

A direct box diagram for the process $e^+e^- \to \mu^+\mu^-$ has the structure given in fig. 12 with $P_5 = p_2 + p_3$ and $P_6 = P_1 + P_2$. The corresponding amplitude is

$$\int d^n q \frac{1}{Q_1Q_2Q_3Q_4}\bar{u}(-p_3)\gamma^\mu(\lambda_1 + \lambda_2\gamma^5)[i(\not{q} + \not{p}_5) + m_3]\gamma^\nu(\lambda_3 + \lambda_4\gamma^5)v(-p_4)$$
$$\times\bar{v}(p_1)\gamma^\nu(\lambda_5 + \lambda_6\gamma^5)(i\not{q} + m_1)\gamma^\mu(\lambda_7 + \lambda_8\gamma^5)u(p_2), \tag{8.1}$$

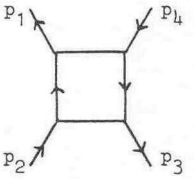

Fig. 12. Direct box diagram.

with*

$$Q_1 = q^2 + m_1^2, \qquad Q_2 = (q+p_2)^2 + m_2^2, \qquad Q_3 = (q+p_2+p_3)^2 + m_3^2,$$
$$Q_4 = (q-p_1)^2 + m_4^2 .$$

By standard methods we can reduce the γ-matrices in the box to a current-current form plus scalar-scalar contributions where the γ are contracted with the momenta such that the Dirac equation cannot be applied anymore.

The crossed box is depicted in fig. 13 with now $p_5 = p_2 + p_4$ and $p_6 = p_1 + p_2$.

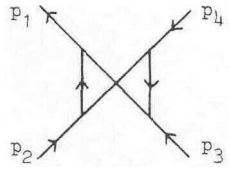

Fig. 13. Crossed **box** diagram.

The amplitude obtains when we make the following substitutions on the direct box:

(i) reversed order for the γ^μ, γ^ν matrices in the muon **line,**

(ii) exchange **of** p_3 and p_4 , which is equivalent to redefinition **of** p_5,

(iii) exchange **of** $\lambda_1 + \lambda_2\gamma^5$ and $\lambda_3 + \lambda_4\gamma^5$,

(iv) an overall minus sign together with $m_3 \to -m_3$.

Six box diagrams are infrared divergent, corresponding to the cases $m_2 = m_4 = \lambda$, $m_2 = \lambda$, $m_4 = \lambda$, for the direct and the crossed box diagrams (λ = photon mass). When $m_2 = 0$ the singularity comes from the poles in $q = -p_2$ while for $m_4 = 0$ the singularity comes from the poles in $q = p_1$. For the integrand we use the decomposition [4]

$$\frac{1}{\prod_i Q_i} = \frac{2}{s - m_2^2 - m_4^2}\left[\frac{(q-p_1)\cdot(q+p_2)}{\prod_i Q_i} - \frac{1}{2\prod_{i\neq 2} Q_i} - \frac{1}{2\prod_{i\neq 4} Q_i}\right]. \tag{8.2}$$

The first term in the right-hand side of eq. (8.2) is not IR divergent and in this way all we need to compute is a 3-point function. For $m_2 = \lambda$, $m_4 = M_0$ we thus find:

$$D_0^{\mathrm{IR}}(p_2, p_3, p_4, m_e, \lambda, m_\mu, M_0) = \frac{1}{-s + M_0^2} C_0^{\mathrm{IR}}(p_2, p_3, m_e, \lambda, m_\mu). \tag{8.3}$$

For $m_2 = M_0$, $m_4 = \lambda$

$$D_0^{\mathrm{IR}}(p_2, p_3, p_4, m_e, M_0, m_\mu, \lambda) = \frac{1}{-s + M_0^2} C_0^{\mathrm{IR}}(p_2 + p_3, p_4, m_e, m_\mu, \lambda). \tag{8.4}$$

Note that p_1, p_2 etc., here **are** not p_1, p_2 etc., **from** the appendix **F,** and **in using** the equations **of** this appendix the appropriate permutation must be made.

Writing

$$C_0^{\mathrm{IR}}(p_2+p_3, p_4, m_e, m_\mu, \lambda)$$
$$= \int \mathrm{d}^n q \frac{1}{(q^2+m_e^2)((q-p_1)^2+\lambda^2)((q-p_1-p_4)^2+m_\mu^2)},$$

we see that in both cases the IR behavior is the same. Indeed, using eqs. (7.6) and (7.7) the result in eq. (8.3) depends on $p_2^2 = -m_e^2$, $p_3^2 = -m_\mu^2$ and α which is a solution of $(p_2+\alpha p_3)^2 = 0$ and on eq, (8.4) on $(-p_1)^2 = -m_e^2$, $(-p_4)^2 = -m_\mu^2$ and on α, solution of $(p_1+\alpha p_4)^2 = 0$. Also:

$$D_0^{\mathrm{IR}}(p_2, p_3, p_4, m_e, \lambda, m_\mu, \lambda) = -\frac{2}{s} C_0^{\mathrm{IR}}(p_2, p_3, m_e, \lambda, m_\mu), \tag{8.5}$$

with [see eq. (7.6)]

$$C_0^{\mathrm{IR}}(p_2, p_3, m_e, \lambda, m_\mu) = \tfrac{1}{2}\tau(t, m_e, m_\mu) \ln \frac{m_e m_\mu}{\lambda^2}. \tag{8.6}$$

Also for the box diagrams we have a complete factorization of the IR divergent part; the numerator of eq. (8.1) near the pole $q = -p_2$ is

$$-\bar{u}\gamma^\mu(\lambda_1+\lambda_2\gamma^5)(\not{q}+\not{p}_5)\gamma^\nu(\lambda_3+\lambda_4\gamma^5)v\bar{v}\gamma^\nu(\lambda_5+\lambda_6\gamma^5)\not{q}\gamma^\mu(\lambda_7+\lambda_8\gamma^5)u$$
$$\simeq 2p_5^2\bar{u}\gamma^\mu(f_{V1}+g_{A1}\gamma^5)v\bar{v}\gamma^\mu(f_{V2}+g_{A2}\gamma^5)u,$$

where in the last step the lepton mass is neglected. Further:

$$f_{V1} = \lambda_1\lambda_3+\lambda_2\lambda_4, \qquad f_{V2} = \lambda_5\lambda_7+\lambda_6\lambda_8,$$
$$g_{A1} = \lambda_1\lambda_4+\lambda_2\lambda_3, \qquad g_{A2} = \lambda_5\lambda_8+\lambda_6\lambda_7.$$

The same result is valid for $q = p_1$; for the crossed box the correspondence rules leave f_{Vi}, g_{Ai} invariant and give an additional minus sign. The result when we specialize to particular diagrams is

$$B_1 \sim i\pi^2 g^4 \frac{s_\theta^2}{-s}\bar{u}\gamma^\mu v\bar{v}\gamma^\mu u 2s_\theta^2 t\tau(t, m_e, m) \ln\frac{m_e m_\mu}{\lambda^2},$$

$$B_2+B_3 \sim i\pi^2 g^4 \frac{1}{16c_\theta^2}\frac{1}{-s+M_0^2}\bar{u}\gamma^\mu(v_\theta-\gamma^5)v\bar{v}\gamma^\mu$$
$$\times(v_\theta-\gamma^5)u 2s_\theta^2 t\tau(t, m_e, m_\mu)\ln\frac{m_e m_\mu}{\lambda^2}.$$

Putting these diagrams together with these of the crossed boxes gives:

$$\mathrm{d}\sigma_{\mathrm{IR}}^{\mathrm{B}} = \frac{g^2}{16\pi^2} 4s_\theta^2[t\tau(t, m_e, m_\mu) - u\tau(u, m_e, m_\mu)]\ln\frac{m_e m_\mu}{\lambda^2}\mathrm{d}\sigma^0. \tag{8.7}$$

The cross-section contribution from box diagrams is

$$d\sigma^{B} = \frac{g^6}{(2\pi)^3}\frac{1}{256}\left(\sigma_{E}^{box} + \frac{1}{c_\theta^2(-s+M_0^2)}\sigma_{W}^{box}\right). \tag{8.8}$$

For each diagram we write:

$$\sigma^{box} = \sigma^{11}D_{11} + \sigma^{12}D_{12} + \sigma^{13}D_{13} + \sigma^{24}D_{24} + \sigma^{25}D_{25} + \sigma^{26}D_{26} + \sigma^{27}D_{27}. \tag{8.9}$$

We found the following relations among the coefficients σ^{ij}

$$\sigma^{13} = -\sigma^{12}, \qquad \sigma^{24} = \sigma^{11} + \sigma^{12},$$

$$\sigma^{25} = -\sigma^{24} - 2\frac{s}{t}\sigma^{12},$$

$$\sigma^{26} = 2\frac{s}{t}\sigma^{12},$$

$$\sigma^{27} = -\frac{2}{t}(\sigma^{11} + 3\sigma^{12}). \tag{8.10}$$

Thus we need only $\sigma_{E,W}^{11}$ and $\sigma_{E,W}^{12}$ for any diagram. We now use the functions defined in sect. 3 and further introduce:

$$Z_1 = -32s_\theta^{12} + 48s_\theta^{10} - 60s_\theta^8 + 40s_\theta^6 - 15s_\theta^4 + 3s_\theta^2 - \tfrac{1}{4},$$
$$Z_2 = -36s_\theta^8 + 36s_\theta^6 - 15s_\theta^4 + 3s_\theta^2 - \tfrac{1}{4},$$
$$Z_3 = -8s_\theta^6 + 12s_\theta^4 - 6s_\theta^2 + 1,$$
$$Z_4 = -32s_\theta^8 + 32s_\theta^6 - 24s_\theta^4 + 8s_\theta^2 - 1,$$
$$v'_\theta = 2s_\theta^2 - 1.$$

Diagram B_1

$$\sigma_E^{11} = 32tx(s,t), \qquad \sigma_E^{12} = 32\frac{t^3}{s^2},$$

$$\sigma_W^{11} = -4s_\theta^4(8s_\theta^4 - v_\theta)stx(s,t) + 4s_\theta^4\frac{t^3}{s},$$

$$\sigma_W^{12} = -16s_\theta^6(2s_\theta^2 - 1)\frac{t^3}{s}.$$

For diagrams B_2 and B_3

$$\sigma_E^{11} = 2s_\theta^2\frac{t}{s}A_I(s,t), \qquad \sigma_E^{12} = 16\frac{s_\theta^6}{c_\theta^2}v'_\theta\frac{t^3}{s^2},$$

$$\sigma_W^{11} = \frac{s_\theta^2}{c_\theta^2} Z_4 stx(s,t) + \frac{s_\theta^2}{c_\theta^2}(1 + 8 s_\theta^2 v'_\theta)\frac{t^3}{s},$$

$$\sigma_W^{12} = -8\frac{s_\theta^6}{c_\theta^2}(4s_\theta^4 - v_\theta)\frac{t^3}{s}.$$

Diagram B_4

$$\sigma_E^{11} = 4 s_\theta^2 \frac{t}{s} A_W(s,t), \qquad \sigma_E^{12} = 8\frac{s_\theta^6}{c_\theta^4}(4s_\theta^4 - v_\theta)\frac{t^3}{s^2},$$

$$\sigma_W^{11} = \frac{1}{c_\theta^4} Z_1 stx(s,t) - \frac{1}{c_\theta^4} Z_2 \frac{t^3}{s}, \qquad \sigma_W^{12} = 4\frac{s_\theta^6}{c_\theta^4} Z_3 \frac{t^3}{s}.$$

Diagram B_5

$$\sigma_E^{11} = 4 s_\theta^2 t\left[x(s,t) - \frac{t^2}{s^2}\right], \qquad \sigma_E^{12} = 0,$$

$$\sigma_W^{11} = (v_\theta - 4s_\theta^4)\left[stx(s,t) - \frac{t^3}{s}\right], \qquad \sigma_W^{12} = 0.$$

Diagram B_6

$d\sigma^B$ for B_6 can be obtained from $d\sigma^B$ for B_1 in the following way

$$t \to u, \qquad \sigma_E^{11} \to -\sigma_E^{11}; \qquad \sigma_E^{12} \to -\sigma_E^{12},$$

$$\sigma_W^{11} = 16 s_\theta^6 (2s_\theta^2 - 1) sux(s,u) + 4 s_\theta^4 \frac{u^3}{s},$$

$$\sigma_W^{12} = 4 s_\theta^4 (8 s_\theta^4 - v_\theta)\frac{u^3}{s}.$$

Diagrams B_7 and B_8

$$\sigma_E^{11} = -16\frac{s_\theta^6}{c_\theta^2} v'_\theta ux(s,u) - 4\frac{s_\theta^4}{c_\theta^2}\frac{u^3}{s^2},$$

$$\sigma_E^{12} = -4\frac{s_\theta^4}{c_\theta^2}(8s_\theta^4 - v_\theta)\frac{u^3}{s^2},$$

$$\sigma_W^{11} = 8\frac{s_\theta^6}{c_\theta^2}(4s_\theta^4 - v_\theta) sux(s,u) + \frac{s_\theta^2}{c_\theta^2}(1 + 8 s_\theta^2 v'_\theta)\frac{u^3}{s},$$

$$\sigma_W^{12} = -\frac{s_\theta^2}{c_\theta^2} Z_4 \frac{u^3}{s}.$$

Diagram B_9

$$\sigma_E^{11} = -8\frac{s_\theta^6}{c_\theta^4}(4s_\theta^4 - v_\theta) ux(s,u) - \frac{s_\theta^2}{c_\theta^4}(1 + 8 s_\theta^2 v'_\theta)\frac{u^3}{s^2},$$

$$\sigma_{\mathrm{E}}^{12} = \frac{s_\theta^2}{c_\theta^4} Z_4 \frac{u^3}{s^2},$$

$$\sigma_{\mathrm{W}}^{11} = -4\frac{s_\theta^6}{c_\theta^4} Z_3 sux(s,u) - \frac{1}{c_\theta^4} Z_2 \frac{u^3}{s},$$

$$\sigma_{\mathrm{W}}^{12} = -\frac{1}{c_\theta^4} Z_1 \frac{u^3}{s}.$$

9. Bremsstrahlung

To the cross section we must add the contribution from $e^+e^- \to \mu^+\mu^-\gamma$ in the soft photon limit; the relevant diagrams are given in fig. 14.

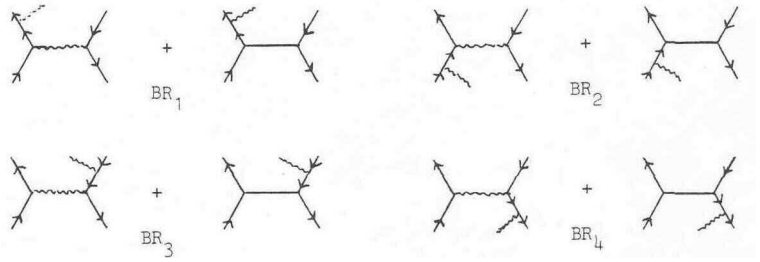

Fig. 14. Bremsstrahlung diagrams.

The photon four-momentum is denoted by k and $\epsilon_\mu(k)$ is the polarization vector; further

$$s_{\mathrm{e}} = -(p_1+p_2)^2, \qquad s_\mu = -(p_3+p_4)^2.$$

We get

$$\mathrm{BR1} \quad (2\pi)^4 ig^3 \left[-\frac{s_\theta^3}{s_\mu} V^\mu V^{\alpha\beta\mu} + \frac{s_\theta}{16c_\theta^2} \frac{1}{-s_\mu + M_0^2} V_5^\mu V_5^{\alpha\beta\mu} \right] \epsilon_\alpha \frac{(p_1+k)_\beta}{2p_1\cdot k},$$

$$\mathrm{BR2} \quad -(2\pi)^4 ig^3 \left[-\frac{s_\theta^3}{s_\mu} V^\mu V^{\mu\beta\alpha} + \frac{s_\theta}{16c_\theta^2} \frac{1}{-s_\mu + M_0^2} V_5^\mu V_5^{\mu\beta\alpha} \right] \epsilon_\alpha \frac{(p_2+k)}{2p_2\cdot k},$$

$$\mathrm{BR3} \quad (2\pi)^4 ig^3 \left[-\frac{s_\theta^3}{s_{\mathrm{e}}} V^{\alpha\beta\mu} V^\mu + \frac{s_\theta}{16c_\theta^2} \frac{1}{-s_{\mathrm{e}} + M_0^2} V_5^{\alpha\beta\mu} V_5^\mu \right] \epsilon_\alpha \frac{(p_3+k)_\beta}{2p_3\cdot k},$$

$$\mathrm{BR4} \quad -(2\pi)^4 ig^3 \left[-\frac{s_\theta^3}{s_{\mathrm{e}}} V^{\mu\beta\alpha} V^\mu + \frac{s_\theta}{16c_\theta^2} \frac{1}{-s_{\mathrm{e}} + M_0^2} V_5^{\mu\beta\alpha} V_5^\mu \right] \epsilon_\alpha \frac{(p_4+k)_\beta}{2p_4\cdot k}, \tag{9.1}$$

$$V^\mu = \bar{u}\gamma^\mu v = \bar{v}\gamma^\mu u, \qquad V_5^\mu = \bar{u}\gamma^\mu(v_\theta - \gamma^5)v = \bar{v}\gamma^\mu(v_\theta - \gamma^5)u,$$
$$V^{\mu\alpha\beta} = \bar{u}\gamma^\mu\gamma^\alpha\gamma^\beta v = \bar{v}\gamma^\mu\gamma^\alpha\gamma^\beta u,$$
$$V_5^{\mu\alpha\beta} = \bar{u}\gamma^\mu(v_\theta - \gamma^5)\gamma^\alpha\gamma^\beta v = \bar{v}\gamma^\mu(v_\theta - \gamma^5)\gamma^\alpha\gamma^\beta u.$$

In the soft photon approximation we put $k \sim 0$ and $s_e = s_\mu = s$; then

$$\mathrm{d}\sigma^{\mathrm{BR}} = \frac{g^2}{16\pi^2}\frac{s_\theta^2}{\pi}\int_{|\boldsymbol{k}|<\omega}\frac{\mathrm{d}^3k}{k_0}\left[\sum_{i=1}^{4}\epsilon_i\frac{p_i}{p_i k}\right]^2 \mathrm{d}\sigma^0. \tag{9.2}$$

The upper limit of integration ω is obtained by considering the photon phase space: we have [2, 4]

$$\omega = -\tfrac{1}{2}\left[E_{\mathrm{th}} - \sqrt{s} + \sqrt{E_{\mathrm{th}}^2 - m_\mu^2} - \frac{m_\mu^2}{E_{\mathrm{th}} - \sqrt{s} - \sqrt{E_{\mathrm{th}}^2 - m_\mu^2}}\right],$$

where E_{th} is the threshold energy at which the muon is detected. In the numerical calculations we used $E_{\mathrm{th}} = 0.45\sqrt{s}$. Further $\epsilon_1 = \epsilon_3 = +1$ and $\epsilon_2 = \epsilon_4 = -1$. By using the results of ref. [3] we obtain the IR divergent part of (9.2)

$$\pi\mathscr{L}_{ij}^{\mathrm{IR}} = p_i p_j \int_{\mathrm{div}}\frac{\mathrm{d}^3k}{k_0}\frac{1}{(p_i\cdot k)(p_j\cdot k)} = 2\pi\bar{\alpha}\frac{p_i p_j}{\bar{\alpha}m_j^2 - m_i^2}\ln\left(\frac{m_j^2}{m_i^2}\bar{\alpha}^2\right)\ln\left(\frac{2\omega}{\lambda}\right)^2, \tag{9.3}$$

where $\bar{\alpha}$ is such that $(p_i - \bar{\alpha}p_j)^2 = 0$. We choose that root for which $\bar{\alpha}p_{j0} - p_{i0}$ has the same sign as p_{i0} and moreover adopt the convention that in eq. (7.7) we take $\alpha = -\bar{\alpha}$. Then

$$\mathscr{L}_{ij}^{\mathrm{IR}} = -2p_i\cdot p_j\tau(s_{ij}, m_i, m_j)\ln\frac{2\omega}{\lambda}, \qquad i \neq j,$$
$$\mathscr{L}_{ii}^{\mathrm{IR}} = -2\ln\frac{2\omega}{\lambda}, \tag{9.4}$$

and we get

$$(\mathrm{d}\sigma^{\mathrm{BR}})_{\mathrm{IR}} = \frac{g^2}{16\pi^2}s_\theta^2\sum_{i,j=1}^{4}(-)^{i+j}\mathscr{L}_{ij}^{\mathrm{IR}}\,\mathrm{d}\sigma^0. \tag{9.6}$$

Infrared divergencies coming from lepton wave function renormalization are canceled by $\sum\mathscr{L}_{ii}^{\mathrm{IR}}$; vertex corrections for the e, μ line by $-2(\mathscr{L}_{12}^{\mathrm{IR}} + \mathscr{L}_{34}^{\mathrm{IR}})$; direct box by $-2(\mathscr{L}_{14}^{\mathrm{IR}} + \mathscr{L}_{23}^{\mathrm{IR}})$; crossed box by $+2(\mathscr{L}_{13}^{\mathrm{IR}} + \mathscr{L}_{24}^{\mathrm{IR}})$. Considering also the finite contributions we have:

$$\mathrm{d}\sigma^{\mathrm{BR}} = \frac{g^2}{8\pi^2}s_\theta^2\sum_{i,j=1}^{4}(-)^{i+j}\mathscr{L}_{ij}\,\mathrm{d}\sigma^0. \tag{9.7}$$

The complete $\mathscr{L}_{ij}$ is for $i=j$ given by

$$\mathscr{L}_{ij} = \mathscr{L}_{ij}^{\mathrm{IR}} - \frac{p_{j0}}{p_j^2 |\boldsymbol{p}_j|} \ln \frac{p_{j0} - |\boldsymbol{p}_j|}{p_{j0} + |\boldsymbol{p}_j|}, \tag{9.8}$$

and for $i \neq j$:

$$\mathscr{L}_{ij} = \mathscr{L}_{ij}^{\mathrm{IR}} - \frac{\bar{\alpha}}{vl}\left[\tfrac{1}{4}\ln^2 \frac{u_0 - |\boldsymbol{u}|}{u_0 + |\boldsymbol{u}|} + \mathrm{Sp}\left(\frac{v + u_0 + |\boldsymbol{u}|}{v}\right) + \mathrm{Sp}\left(\frac{v + u_0 - |\boldsymbol{u}|}{v}\right)\right]_{u=p_j}^{u=\alpha p_i}, \tag{9.9}$$

where

$$l = \bar{\alpha} p_{j0} - p_{i0}, \qquad v = \frac{1}{l} p_i (\bar{\alpha} p_j - p_i),$$

$\bar{\alpha}$ solution **of** $(p_i - \bar{\alpha} p_j)^2 = 0$, sign $(\bar{\alpha} p_{j0} - p_{i0}) = \mathrm{sign}\,(p_{i0})$.

10. Renormalization

The one-loop corrections we have computed are ultraviolet divergent and the amplitude includes poles in $n-4$ which must be renormalized away while a finite part must be fixed in a unique way.

In principle renormalization is achieved as follows. The model contains a number of free parameters, and we need as many data points to fix these parameters. The requirement is that the parameters are such that lowest order plus radiative corrections produce the correct result. Evidently the parameters in the Lagrangian change as higher and higher order corrections are taken into account. For instance, in lowest order we will obtain for some coupling constant g the value go, including one-loop corrections we must choose $g = g_0 + \delta g$, etc.

Clearly, it is of no importance which data points are taken to fix our parameters. In practice we are limited by the complications that a given choice induces. The ideal choice at this moment would be to take the lifetime of the muon, the electric charge of the electron and the weak mixing angle as observed at low energy as the three data points. However this would imply that we must compute the radiative corrections to μ-decay, to e-e scattering and to ν-e or ν-quark scattering, which is a bit too much for the moment. Instead we have chosen the following procedure. We take it for granted that the values of the masses of the charged and neutral vector boson as deduced from the usual lowest-order relations are close to their actual value. Thus we assume as experimental data the mass values $M_0 = 90$ GeV and M = 79.5 GeV for the neutral and charged vector boson respectively. Admittedly, this is not the ideal thing to do, and perhaps we are missing some very interesting radiative corrections to the vector boson masses, but for the moment we must postpone investigations on this point. The third data point obtains by requiring that at low energy the results of QED must be reproduced; we simply take one

point from the calculation of Berends et al., ref. [6] and consider that as our third experimental result. Of course the consistency of this procedure can be checked by comparing subsequently with other points at low energies. As a matter of record we note here that there is perfect agreement, in fact we always get the same results in all regions independent of which data point we choose from the work of Berends et al. [6].

We thus introduce the quantity δM^2 into the Lagrangian, and consider the W^+ self-energy contributions, fig. 15. We now set δM^2 to that value that makes the total contribution of these diagrams zero at $s = M^2$. We obtain (see sect. 5):

$$\delta M^2 = \frac{g^2}{16\pi^2} A^+(M^2) . \tag{10.1}$$

The Lagrangian contains further the parameters g, g_1, g_2, g_3. However as noted before g_2 and g_3 are not free and we are left with the free parameters g and g_1. The relations that we have proved in sect. 7 show the consistency of this scheme. Thus we now replace g_1 by $g_1 + \delta g_1$ in the Lagrangian, and subsequently fix δg_1 by the requirement that the W° mass equals its lowest-order value. Now s_θ is directly related to g_1 and we actually used the quantity δs_θ^2. We obtain:

$$\delta s_\theta^2 = c_\theta^2 \left(\frac{\delta M_0^2}{M_0^2} - \frac{\delta M^2}{M^2} \right) , \tag{10.2}$$

with (see sect. 5):

$$\delta M_0^2 = \frac{g^2}{16\pi^2} A^0(M_0^2) .$$

Our third parameter is the electric charge, $e = g s_\theta$. It must be fixed by comparison with the low-energy QED results. But first we must add terms that arise from δs_θ^2; this amounts to adding

$$\mathrm{d}\sigma_\theta^{\mathrm{ren}} = \delta s_\theta^2 \frac{\partial}{\partial s_\theta^2} (\sigma_{\mathrm{W}}^0 + \sigma_{\mathrm{I}}^0) . \tag{10.3}$$

In eq. (10.3) the lowest-order cross section must be expressed in terms of e, s_θ and M_0^2, substituting $g = e/s_\theta$ everywhere.

Finally we replace in $\mathscr{L}$ the electric charge by $e + \delta e$, and fix δe by the requirement that the cross section for some value of s and t takes a specified value. For

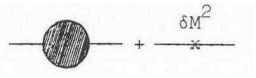

Fig. 15. W^+ self-energy.

that we use the results of ref. [6] in the low-energy region under the assumption that there the e.m. corrections dominate. Inclusion **of** the δe terms in the cross section completes our renormalization procedure.

In order to show the self-consistency of this procedure we have to analyze the cancellation of ultraviolet divergencies and the independence of the finite parts on the units that masses are expressed in. These two features always **go** together and are typical for the renormalization procedures; indeed by inspection the ultraviolet divergent form factors are ***A, BO,*** B_1, B_{21}, B_{22}, C_{24} and they do not scale properly due to occurrence **of** In ***M*** terms. **As a** consequence the quantities δM^2, δs_θ^2 and δe depend on the units chosen. But after addition **of** the counter term $d\sigma_\theta^{\text{ren}}$ and an analogous expression involving δe there is no scale dependence of the results. In fact this provides a powerful check on the whole calculation and the renormalization procedure.

11. Results

Using the Weinberg model for weak and e.m. interactions we have carried through a calculation of higher order effects in the process $e^+e^- \to \mu^+\mu^-$. In this calculation we have neglected terms proportional to the lepton mass, which is of very little consequence and furthermore we have not taken into account the finite width of the W°. This width is of course unknown, we have computed 480.8 MeV, made up from $2\Gamma_{\nu\nu} + \Gamma_{ee} + \Gamma_{\mu\mu} = 319 + 80.9 + 80.9$ MeV, for $\sin^2\theta = 0.22$. Also this approximation is of little consequences except very near to the W° resonance (say within 5 GeV). Finally we have not considered hard bremsstrahlung.

At low energies W^0 exchange is negligible but at energies comparable to *MO* where weak interactions start to dominate all the one-loop corrections have to be considered together. Using the formulas we have developed in the previous sections we have computed the radiative corrections to the $e^+e^- \to \mu^+\mu^-$ cross section up to terms $O(g^6)$ from 40-200 GeV e.m. energy. For the Higgs mass we have taken 200 GeV; the W° mass is given by:

$$M_0^2 = \tfrac{1}{2}\pi\alpha \sin^{-2}\theta \cos^{-2}\theta G_F^{-1} \sim (90\ \text{GeV})^2 ,$$

where G_F is the Fermi coupling constant and $\sin^2\theta = 0.22$, which value we have used throughout. The numerical analysis gives a good agreement for the pure QED process with the results of refs. [4] and [6]. As noted before we have used one point from their calculations to fix our δe; all other points that we have checked on agree excellently. Furthermore we have computed the QED corrections according to the equations given in refs. [4,6] and compared with the contributions of the appropriate diagrams of our calculation, with excellent agreement. For the photon mass λ in the numerical calculations we have used different values of keV order and the results are stable against variations of λ. Furthermore our results are invariant against variations in Δ, the quantity substituted for $1/n-4$ in the various

divergent functions. **This shows** that both the infrared and the ultraviolet divergences **have** been treated correctly and that the necessary identities are fulfilled by **our** numerical expressions. Results are given in tables 1-3.

Table 1
Lowest-order cross section for $e^+e^- \to \mu^+\mu^-$ in 10^{-2} nb

θ_s \ $\sqrt{s}$	44	48	52	56	60	64	68	72	76	80	84
20°	2.48	1.94	1.51	1.16	0.86	0.59	0.36	0.17	0.06	0.25	2.25
60°	1.74	1.39	1.11	0.89	0.70	0.54	0.41	0.31	0.29	0.50	2.01
120°	2.51	2.20	1.99	1.83	1.74	1.71	1.75	1.81	2.27	3.18	6.23
160°	3.92	3.47	3.15	2.94	2.82	2.80	2.89	3.17	3.79	5.29	10.17

θ_s \ $\sqrt{s}$	100	104	108	112	116	120	130	140	160	180	200
20°	5.45	3.53	2.61	2.07	1.72	1.46	1.07	0.84	0.57	0.42	0.32
60°	3.29	2.12	1.56	1.24	1.03	0.88	0.64	0.50	0.35	0.26	0.20
120°	0.65	0.30	0.18	0.14	0.12	0.11	0.92	0.84	0.70	0.59	0.50
160°	0.49	0.11	0.19[a)]	0.02	0.06	0.15	0.36	0.48	0.54	0.52	0.47

a) In 10^{-3} nb.

Table 2
Percentage corrections in QED for $e^+e^- \to \mu^+\mu^-$

θ_s \ $\sqrt{s}$	30	44	56	68	80	100	120	140	200
20°	−7.92	−8.79	−9.34	−9.78	−10.15	−10.66	−11.07	−11.42	−12.23
60°	−11.78	−14.94	−15.48	−15.92	−16.29	−16.80	−17.21	−17.56	−18.37
120°	−16.23	−20.06	−20.61	−21.05	−21.48	−21.92	−22.33	−22.68	−23.49
160°	−21.48	−26.19	−26.47	−27.18	−27.55	−28.06	−28.47	−28.82	−29.63

Table 3
Percentage corrections in the Weinberg model for $e^+e^- \to \mu^+\mu^-$

θ_s \ $\sqrt{s}$	44	48	52	56	60	64	68	72	76	80	84
20°	−8.15	−8.13	−8.02	−7.76	−7.27	−6.37	−4.65	−1.52	−11.29	−32.63	−26.05
60°	−14.62	−14.74	−14.81	−14.84	−14.83	−14.76	−14.71	−14.99	−16.69	−19.77	−21.13
120°	−19.73	−19.88	−20.00	−20.10	−20.18	−20.24	−20.27	−20.26	−20.20	−20.05	−19.70
160°	−25.60	−25.67	−25.70	−25.68	−25.61	−25.46	−25.23	−24.85	−24.26	−23.30	−21.61

θ_s \ $\sqrt{s}$	100	104	108	112	116	120	130	140	160	180	200
20°	−15.16	−14.24	−13.72	−13.42	−13.25	−13.16	−13.17	−13.39	−15.06	−14.58	−14.09
60°	−18.59	−18.32	−18.19	−18.14	−18.14	−18.16	−18.27	−18.43	−18.73	−19.04	−19.44
120°	−21.04	−21.73	−22.18	−22.41	−22.48	−22.49	−22.46	−22.41	−21.35	−23.00	−24.00
160°	−18.07	−16.46	−11.76	−20.76	−40.20	−34.28	−30.21	−29.21	−28.69	−28.42	−28.76

$\sqrt{s}$ in GeV. Further $\sin^2\theta = 0.22$, $M = 79.5$ and $M_0 = 90$ GeV. Higgs mass = 200 GeV.

To present the results of our calculations we take as a starting point the QED predictions for $e^+e^- \to \mu^+\mu^-$; the lowest-order cross sections is a monotonously decreasing function of 5. Working in the context of the Weinberg model we know already what can be expected from inclusion of weak interactions in lowest order, namely the largest effect in the cross section is due to the W^0 (which is at 90 GeV for our choice of $\sin^2\theta$), while in the angular distribution a forward-backward asymmetry is introduced. We will now present the radiative corrections to the QED and QED + WEAK process; and we will be particularly interested in the regions where the corrections to the QED + WEAK process differ from what is suggested by a pure e.m. theory, in particular soft photon contributions. We consider these somewhat less interesting because they are process independent and simply proportional to the lowest-order cross section. To this purpose we have taken from our numerical calculations the pure QED part and considered the percentage corrections for different values of the scattering angle in a range of the energy from 30 to 200 GeV. The conclusion is that with our choice of the infrared cutoff ω (see sect. 9) they are slowly increasing with the energy (a difference of 4% for $\theta_s \sim 0$ and of 8% for $\theta_s \sim \pi$, over the range of the energies that we have investigated) and they become larger for increasing θ_s. This behavior introduces by itself an asymmetry which can be described by a function $A(s, \theta_s)$ given by

$$A(s, \theta_s) = \mathrm{d}\sigma(s, \theta_s) - \mathrm{d}\sigma(s, \pi - \theta_s)\,, \tag{11.1}$$

which remains positive for all values of s. The QED cross section can be written as

$$\mathrm{d}\sigma_{\mathrm{QED}} = \mathrm{d}\sigma^0_{\mathrm{QED}}(1 + \delta_s) + \mathrm{d}\sigma^{\mathrm{H}}_{\mathrm{QED}}\,, \tag{11.2}$$

where $\mathrm{d}\sigma^0_{\mathrm{QED}}$ is the lowest-order cross section and δ_s is the percentage correction due to soft photons. As noted before this can be seen as a property of external lines since it corresponds to a factorization in the bremsstrahlung and in the part of the virtual corrections in which the internal photon line is near the mass shell. Further $\mathrm{d}\sigma^{\mathrm{H}}_{\mathrm{QED}}$ is then the hard photon cross section which does not factorize, and it can be prominent if the lowest-order cross section is very small in some region.

We are now in a position to compare these results with the radiative corrections in the Weinberg model; we investigate their effects both for s fixed and for θ_s fixed. In the first case the behavior of the cross section as a function of the scattering angle is better analyzed in terms of the asymmetry A defined in eq. (11.1). $A(s, \theta_s)$ is negative for s less than M_0^2 and it changes sign after the peak. Since the W^0 width has not been included we have limited ourselves to the regions of 40-80 GeV and of 100-200 GeV. Moreover the absolute value of A increases with s in the region to the left of the peak, while behind the peak itself A starts to decrease rapidly. We turn to the behavior for fixed θ_s of the radiative corrections; our results do not differ very much from what is expected from QED when θ_s is in the central region. There the percentage corrections change slowly with s and apart from small

fluctuations they resemble the QED results, provided we are away from the W° resonance. To be more precise we can say that below the pole of the W° and for $\theta_s \geqslant 50°$ and above it for $\theta_s \leqslant 150°$ there is no drastic departure from a QED like behavior. Moreover for very high energy the percentage corrections are within 2% the same as in pure QED, independently from θ_s. Brief, away from the W° resonance the radiative corrections are dominated by soft photons, and thus process independent. We can distinguish then four different regions

$$\text{I} \quad s < M_0^2,\ \theta_s \leqslant 50°; \qquad \text{II} \quad s < M_0^2,\ \theta_s \geqslant 50°;$$
$$\text{III} \quad s > M_0^2,\ \theta_s \leqslant 150°; \qquad \text{IV} \quad s > M_0^2,\ \theta_s \geqslant 150°.$$

To give an idea of the behavior we list a few examples; in QED for $\theta_s = 120°$ the percentage corrections are almost constant (going from -21% to -23%) from 40 to 200 GeV. This can be compared with QED + WEAK where we have a constant -20% before the peak, which changes into a -22% after it and starts to increase to a value of -24% for 200 GeV. When we move away from the central region in θ_s toward regions I or IV the situation becomes slightly different; for instance if we approach region I the percentage corrections show the following behavior. They increase with s up to some value, then they go down having a minimum, to increase again with a larger slope. For values of θ_s near the boundary between regions I and II this effect is still very small and of little consequence.

To give an example of this we consider QED for $\theta_s = 60°$ where the percentage corrections go from -15% at 40 GeV to -16% at 80 GeV and further increase for higher energy, finally reaching -18% for 200 GeV. Taking into account weak interactions for the same value of θ_s we get an average of -14% in the region of 40-72 GeV. The percentage correction starts to increase around 76 GeV to a maximum value of -21% to go back after the W° peak at a -18%, which remains stable. This phenomenon is the first signal for a departure from QED. It appears for small scattering angles in a range of energy of a few GeV before the resonance (inside region I) and also for big scattering angles behind that (inside region IV). Again we can write the cross section as

$$\mathrm{d}\sigma = \mathrm{d}\sigma^0(1+\delta_s) + \mathrm{d}\sigma^{\mathrm{H}},$$

where δ_s is the same as in eq. (11.2). Now the lowest-order cross section shows a novel feature when the c.m. energy is around 76 GeV in the forward direction and around 114 GeV in the backward direction; there the weak part is of the same order of magnitude as the e.m. part and the interference is totally destructive, lowering the cross section to 6% and 0.4% respectivley of the pure QED result. As a consequence of this the hard photon part $\mathrm{d}\sigma^{\mathrm{H}}$ has a chance to show up and turns out to be up to 32% from 73 to 80 GeV for $0_S = 20°$ and up to 40% from 110 to 114 GeV for $\theta_s = 160°$. Outside this range of the energy also for values of θ_s near to π c.q. 0 nothing differs from a QED-like behavior, dominated by soft photon

contributions. In connection with these interesting regions we notice again that only the soft photon part of the bremsstrahlung integral has been taken into account and to be complete we should integrate the exact bremsstrahlung cross section over the isotropic and anisotropic part of the photon phase space. In other words hard bremsstrahlung may be important here.

We may conclude that away from regions where the lowest-order cross section becomes very small the soft photons completely dominate the radiative corrections. In certain regions where the lowest-order cross section is very small, due to weak-e.m. interference, effects not due to soft photons become visible. Perhaps these effects are within experimentally possibilities, and then they would constitute a very interesting test of the theory. However, we wish to emphasize that the hard bremsstrahlung effects have not yet been included. Since these bremsstrahlung effects may also be particularly large in the regions mentioned they certainly should be considered.

The authors gratefully acknowledge stimulating discussions with Drs. Berends, Gaemers, Gastmans and Lemoine. They are also indebted to Dr. M. Consoli, for an independent check of our numerical results. One of the authors (G.P.) would like to acknowledge the financial support of the "Istituto Nazionale di Fisica Nucleare" (INFN).

Appendix A

The Lagrangian for the Weinberg model

In this appendix we give the complete expression for the Lagrangian $\mathscr{L}_T$ in terms of the fields W^0_μ, A_μ, $W^\pm_\mu$, Z, $\phi^\pm$, ϕ^0. Using (2.2), (2.4), (2.6) and the following definitions

$$M = \sqrt{\tfrac{1}{2}}gF, \qquad \alpha = \lambda/g^2, \qquad \beta = \mu + \lambda F^2, \qquad m^2 = 4\alpha M^2, \tag{A.I}$$

we get

$$\mathscr{L}_T = \mathscr{L}_{YM} + \mathscr{L}_K + \mathscr{L}_{g.f.} + \mathscr{L}_{fermion},$$

$$\begin{aligned}
\mathscr{L}_T = &- W^+_{\mu,\nu}W^-_{\mu,\nu} - M^2 W^+_\mu W^-_\mu - \tfrac{1}{2}W^0_{\mu,\nu}W^0_{\mu,\nu} - \tfrac{1}{2}\frac{M^2}{c_\theta^2}W^0_\mu W^0_\mu - \tfrac{1}{2}A_{\mu,\nu}A_{\mu,\nu} \\
&- \phi^+_{,\mu}\phi^-_{,\mu} - M^2\phi^+\phi^- - \tfrac{1}{2}\phi^0_{,\mu}\phi^0_{,\mu} - \tfrac{1}{2}\frac{M^2}{c_\theta^2}\phi^0\phi^0 - \tfrac{1}{2}Z_{,\mu}Z_{,\mu} - \tfrac{1}{2}m^2Z^2 \\
&- ic_\theta\{W^0_{\mu,\nu}W^{[+}_\mu W^{-]}_\nu - W^0_\nu W^{[+}_\mu W^{-]}_{\mu,\nu} + W^0_\mu W^{[+}_\nu W^{-]}_{\mu,\nu}\} \\
&- is_\theta\{A_{\mu,\nu}W^{[+}_\mu W^{-]}_\nu - A_\nu W^{[+}_\mu W^{-]}_{\mu,\nu} + A_\mu W^{[+}_\nu W^{-]}_{\mu,\nu}\} \\
&- \tfrac{1}{2}(W^+_\mu W^-_\mu)^2 + \tfrac{1}{2}(W^+_\mu W^-_\nu)^2 + c_\theta^2\{W^0_\mu W^+_\mu W^0_\nu W^-_\nu - W^0_\mu W^0_\mu W^+_\nu W^-_\nu\}
\end{aligned}$$

$$
\begin{aligned}
&+s_\theta^2\{A_\mu W_\mu^+ A_\nu W_\nu^- - A_\mu A_\mu W_\nu^+ W_\nu^-\}\\
&+s_\theta c_\theta\{A_\mu W_\nu^0(W_\mu^+ W_\nu^- + W_\nu^+ W_\mu^-) - 2A_\mu W_\mu^0 W_\nu^+ W_\nu^-\}\\
&-2\beta M^2 - 2\beta MZ - \tfrac{1}{2}\beta(Z^2+\phi^{02}+2\phi^+\phi^-) + 2M^4\alpha\\
&-\alpha MZ\{Z^2+\phi^{02}+2\phi^+\phi^-\}\\
&-\tfrac{1}{8}\alpha\{Z^4+\phi^{04}+4\phi^+\phi^-\phi^+\phi^- + 4\phi^{02}\phi^+\phi^- + 4Z^2\phi^+\phi^- + 2\phi^{02}Z^2\}\\
&-MZW_\mu^+W_\mu^- - \tfrac{1}{2}\frac{M}{c_\theta^2}ZW_\mu^0W_\mu^0\\
&-\tfrac{1}{2}i\{W_\mu^+(\phi^0\phi_{,\mu}^- - \phi^-\phi_{,\mu}^0) - W_\mu^-(\phi^0\phi_{,\mu}^+ - \phi^+\phi_{,\mu}^0)\}\\
&+\tfrac{1}{2}\{W_\mu^+(Z\phi_{,\mu}^- - \phi^- Z_{,\mu}) + W_\mu^-(Z\phi_{,\mu}^+ - \phi^+ Z_{,\mu})\}\\
&+\tfrac{1}{2}\frac{1}{c_\theta}\{W_\mu^0(Z\phi_{,\mu}^0 - \phi^0 Z_{,\mu})\}\\
&-i\frac{s_\theta^2}{c_\theta}MW_\mu^0(W_\mu^+\phi^- - W_\mu^-\phi^+) + is_\theta MA_\mu(W_\mu^+\phi^- - W_\mu^-\phi^+)\\
&-i\frac{(\frac{1}{2}-c_\theta^2)}{c_\theta}W_\mu^0(\phi^+\phi_{,\mu}^- - \phi^-\phi_{,\mu}^+) + is_\theta A_\mu(\phi^+\phi_{,\mu}^- - \phi^-\phi_{,\mu}^+)\\
&-\tfrac{1}{4}W_\mu^+W_\mu^-(Z^2+\phi^{02}+2\phi^+\phi^-)\\
&-\tfrac{1}{8}\frac{1}{c_\theta^2}W_\mu^0W_\mu^0(Z^2+\phi^{02}+2(2s_\theta^2-1)^2\phi^+\phi^-) - s_\theta^2A_\mu A_\mu\phi^+\phi^-\\
&-\tfrac{1}{2}\frac{s_\theta^2}{c_\theta}W_\mu^0\phi^0(W_\mu^+\phi^- + W_\mu^-\phi^+) - \tfrac{1}{2}i\frac{s_\theta^2}{c_\theta}W_\mu^0Z(W_\mu^+\phi^- - W_\mu^-\phi^+)\\
&+\tfrac{1}{2}s_\theta A_\mu\phi^0(W_\mu^+\phi^- + W_\mu^-\phi^+) + \tfrac{1}{2}is_\theta A_\mu Z(W_\mu^+\phi^- - W_\mu^-\phi^+)\\
&-\frac{s_\theta}{c_\theta}(2c_\theta^2-1)W_\mu^0A_\mu\phi^+\phi^- - \bar\nu\partial\!\!\!/\nu - \bar l(\partial\!\!\!/ + m_\ell)l\\
&+\frac{i}{4c_\theta}\bar\nu\gamma^\mu(1+\gamma^5)\nu W_\mu^0 + \frac{i}{2\sqrt2}\bar\nu\gamma^\mu(1+\gamma^5)lW_\mu^+ + \frac{i}{2\sqrt2}\bar l\gamma^\mu(1+\gamma^5)\nu W_\mu^-\\
&-\frac{i}{2\sqrt2}\frac{m_\ell}{M}\bar\nu(1-\gamma^5)l\phi^+ + \frac{i}{2\sqrt2}\frac{m_\ell}{M}\bar l(1+\gamma^5)\nu\phi^- - \tfrac{1}{2}\frac{m_\ell}{M}\bar llZ - \tfrac{1}{2}i\frac{m_\ell}{M}\bar l\gamma^5 l\phi^0\\
&+\frac{i}{4c_\theta}\bar l\gamma^\mu(4s_\theta^2-1-\gamma^5)lW_\mu^0 - is_\theta\bar l\gamma^\mu lA_\mu,
\end{aligned}
$$

where $x_{,\mu} = \partial_\mu x$ and $x^{[a}y^{b]} = x^a y^b - x^b y^a$.

To every term with three fields a factor g should be added and to a term with four fields a factor g^2; and terms with one field require a factor $1/g$.

For $\mathscr{L}_{\text{ghost}}$ we introduce the fields X^a, X^0 $(a = 1, 2, 3)$; further

$$X^3 = c_\theta Y^0 + s_\theta Y^A,$$
$$X^0 = -s_\theta Y^0 + c_\theta Y^A,$$
$$X^1 = \sqrt{\tfrac{1}{2}}(X^+ + X^-),$$
$$X^2 = \sqrt{\tfrac{1}{2}} i(X^+ - X^-),$$
$$\mathscr{L}_{\text{ghost}} = \bar{X}^+\partial^2 X^+ - M^2\bar{X}^+X^+ + \bar{X}^-\partial^2 X^- - M^2\bar{X}^-X^- + \bar{Y}^0\partial^2 Y^0$$
$$-\frac{M^2}{c_\theta^2}\bar{Y}^0 Y^0 + \bar{Y}^A\partial^2 Y^A$$
$$-is_\theta W_\mu^+(\partial_\mu\bar{X}^+Y^A - \partial_\mu\bar{Y}^AX^-) + ic_\theta W_\mu^+(\partial_\mu\bar{Y}^0X^- - \partial_\mu\bar{X}^+Y^0)$$
$$-is_\theta W_\mu^-(\partial_\mu\bar{Y}^AX^+ - \partial_\mu\bar{X}^-Y^A) + ic_\theta W_\mu^-(\partial_\mu\bar{X}^-Y^0 - \partial_\mu\bar{Y}^0X^+)$$
$$-is_\theta A_\mu(\partial_\mu\bar{X}^-X^- - \partial_\mu\bar{X}^+X^+) - ic_\theta W_\mu^0(\partial_\mu\bar{X}^-X^- - \partial_\mu\bar{X}^+X^+)$$
$$-\tfrac{1}{2}MZ(\bar{X}^+X^+ + \bar{X}^-X^- + \frac{1}{c_\theta^2}\bar{Y}^0Y^0)$$
$$+i\frac{(\frac{1}{2}-c_\theta^2)}{c_\theta}M(\bar{X}^+Y^0\phi^+ - \bar{X}^-Y^0\phi^-)$$
$$+i\tfrac{1}{2}\frac{M}{c_\theta}(\bar{Y}^0X^-\phi^+ - \bar{Y}^0X^+\phi^-)$$
$$-is_\theta M(\bar{X}^+Y^A\phi^+ - \bar{X}^-Y^A\phi^-)$$
$$-\tfrac{1}{2}iM(\bar{X}^-X^- - \bar{X}^+X^+)\phi^0.$$

In terms of the fields used above the gauge fixing functions C^a are:

$$C^+ = -\partial_\mu W_\mu^+ + M\phi^+,$$
$$C^- = -\partial_\mu W_\mu^- + M\phi^-,$$
$$C^3 = -c_\theta\partial_\mu W_\mu^0 - s_\theta\partial_\mu A_\mu + \frac{M}{c_\theta}\phi^0,$$
$$C^A = s_\theta\partial_\mu W_\mu^0 - c_\theta\partial_\mu A_\mu.$$

Appendix B

In $e^+e^- \to \mu^+\mu^-$ like **in** all the other processes in which there are no external vector lines the coupling of Z, ϕ^0, $\phi^\pm$ to a fermionic current is suppressed by a factor m_ℓ/M ($\sim 10^{-5}$ for the electron, $\sim 10^{-3}$ for the muon) and we neglect it systematically.

For one-loop diagrams the following vertices will be relevant:

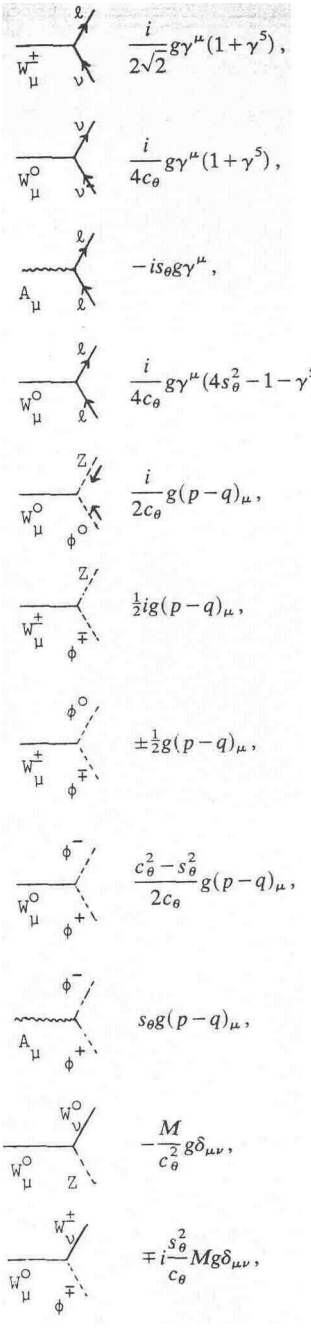

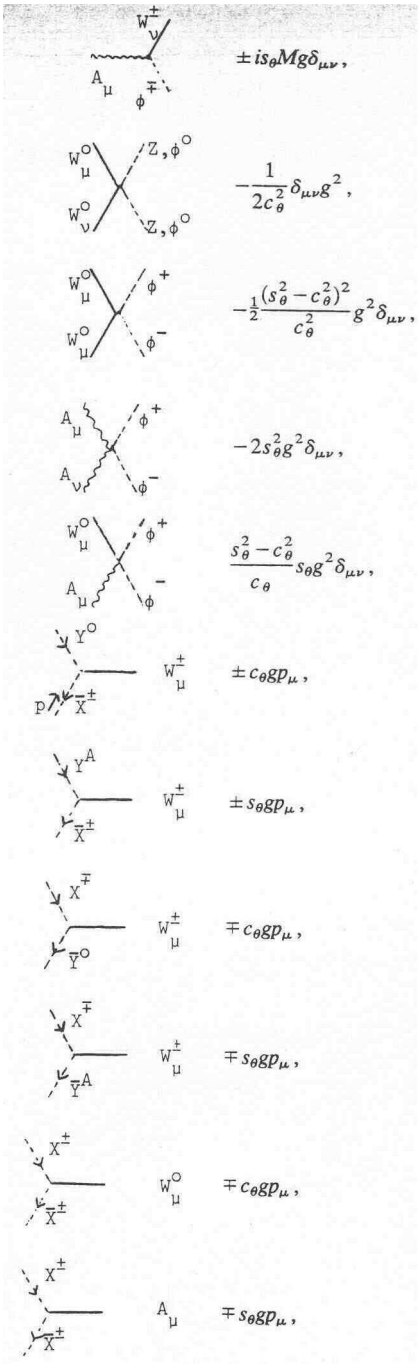
$\pm is_\theta Mg\delta_{\mu\nu}$,
$-\frac{1}{2c_\theta^2}\delta_{\mu\nu}g^2$,
$-\frac{1}{2}\frac{(s_\theta^2-c_\theta^2)^2}{c_\theta^2}g^2\delta_{\mu\nu}$,
$-2s_\theta^2 g^2\delta_{\mu\nu}$,
$\frac{s_\theta^2-c_\theta^2}{c_\theta}s_\theta g^2\delta_{\mu\nu}$,
$\pm c_\theta g p_\mu$,
$\pm s_\theta g p_\mu$,
$\mp c_\theta g p_\mu$,
$\mp s_\theta g p_\mu$,
$\mp c_\theta g p_\mu$,
$\mp s_\theta g p_\mu$,

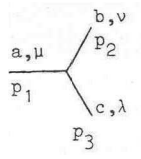

$$-ig\epsilon_{abc}[\delta_{\mu\lambda}(p_1-p_3)_\nu+\delta_{\lambda\nu}(p_3-p_2)_\mu+\delta_{\nu\mu}(p_2-p_1)_\lambda],$$

with $\epsilon_{3+-}=-i, \qquad \epsilon_{3-+}=+i.$

The index 3 refers to $W^3_\mu = c_\theta W^0_\mu + s_\theta A_\mu$

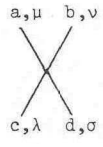

$$-g^2[\epsilon_{edc}\epsilon_{eba}(2\delta_{\mu\lambda}\delta_{\nu\sigma}-\delta_{\mu\sigma}\delta_{\nu\lambda}-\delta_{\mu\nu}\delta_{\lambda\sigma})$$
$$+\epsilon_{edb}\epsilon_{eca}(2\delta_{\mu\nu}\delta_{\lambda\sigma}-\delta_{\mu\sigma}\delta_{\nu\lambda}-\delta_{\mu\lambda}\delta_{\nu\sigma})].$$

The last diagram is equivalent to

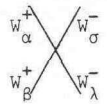

$$g^2(2\delta_{\alpha\beta}\delta_{\lambda\sigma}-\delta_{\alpha\lambda}\delta_{\beta\sigma}-\delta_{\alpha\sigma}\delta_{\beta\lambda})$$

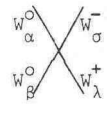

$$-g^2c_\theta^2(2\delta_{\alpha\beta}\delta_{\lambda\sigma}-\delta_{\alpha\lambda}\delta_{\beta\sigma}-\delta_{\alpha\sigma}\delta_{\beta\lambda})$$

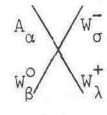

$$-g^2s_\theta c_\theta(2\delta_{\alpha\beta}\delta_{\lambda\sigma}-\delta_{\alpha\lambda}\delta_{\beta\sigma}-\delta_{\alpha\sigma}\delta_{\beta\lambda})$$

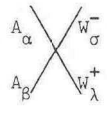

$$-g^2s_\theta^2(2\delta_{\alpha\beta}\delta_{\lambda\sigma}-\delta_{\alpha\lambda}\delta_{\beta\sigma}-\delta_{\alpha\sigma}\delta_{\beta\lambda})$$

Propagators:

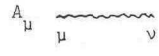

$$\frac{\delta_{\mu\nu}}{p^2-i\epsilon}$$

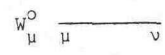

$$\frac{\delta_{\mu\nu}}{p^2+M_0^2-i\epsilon}$$

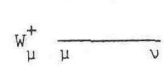

$$\frac{\delta_{\mu\nu}}{p^2+M^2-i\epsilon}$$

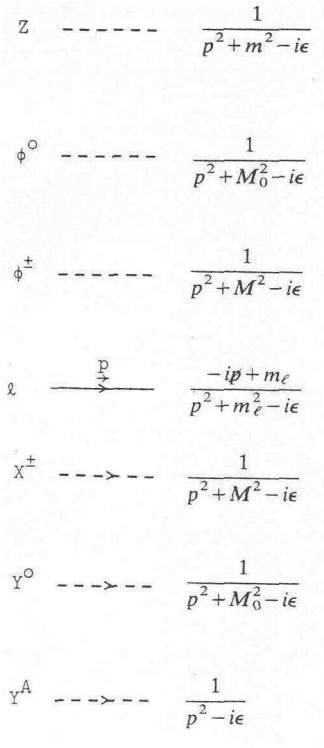

Appendix C

Diagrams

Diagrams which contribute to the amplitude $e^+e^- \to \mu^+\mu^-$, or to the Ward identities are:

Photon self-energy:

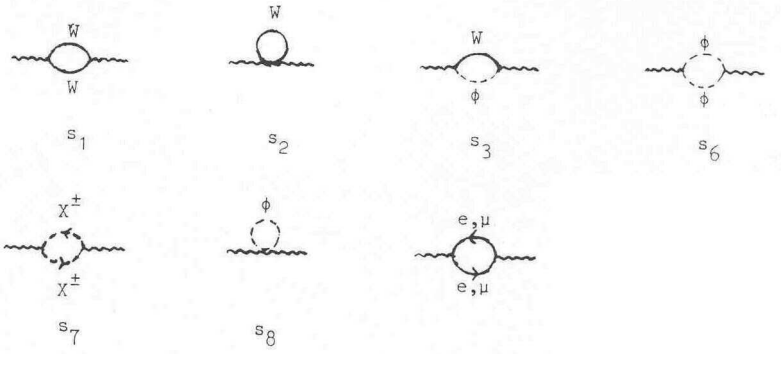

W° self-energy:

We have the same types of diagrams as in the photon self-energy with external W° lines and in addition:

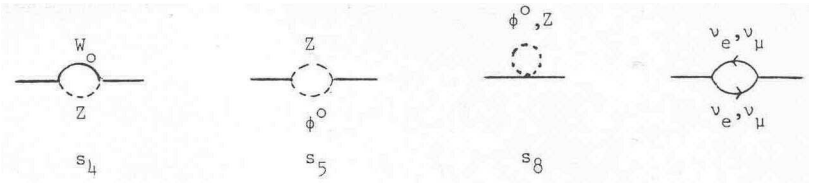

Photon - W transition:

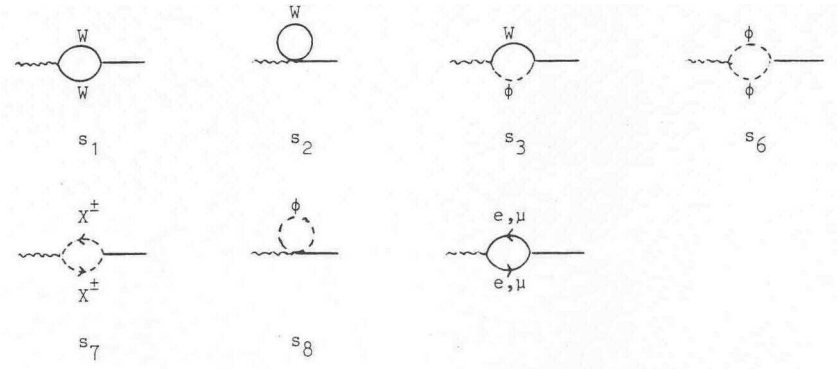

W^+ self-energy:

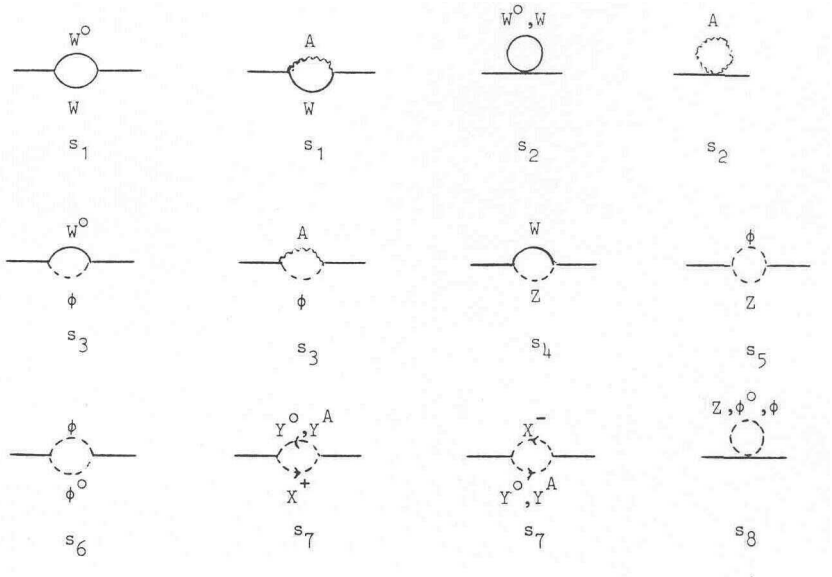

e, μ self-energy:

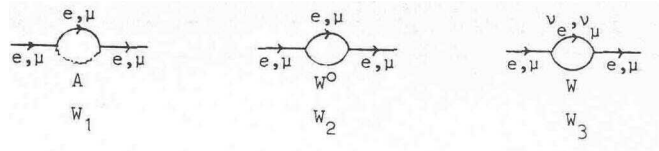

tadpoles:

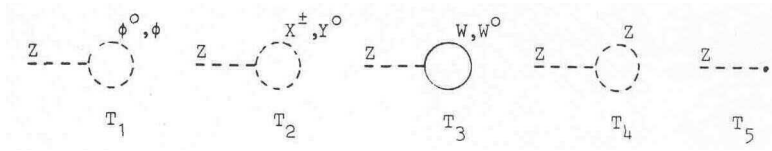

ϕ^+ *self-energy:*

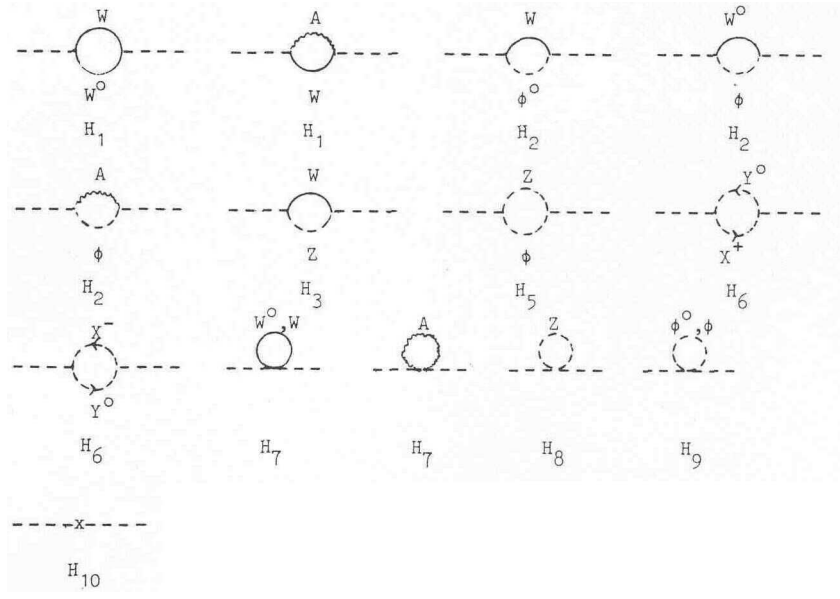

ϕ^o *self-energy:*

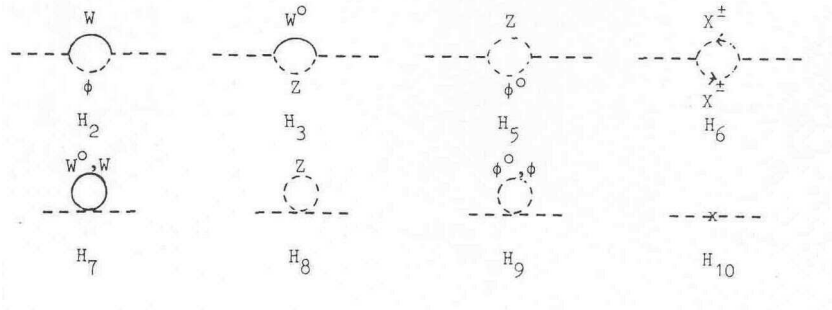

$\phi - W$ transition:

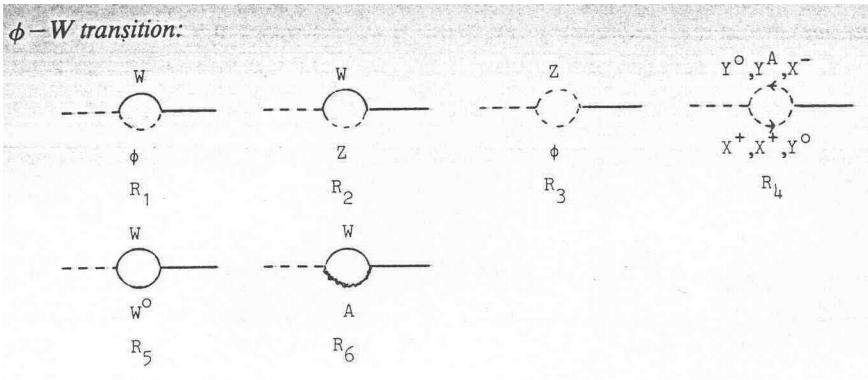

$\phi^o - W^o$ transition:

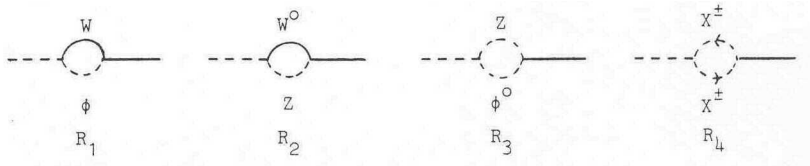

ϕ^o-A transition:

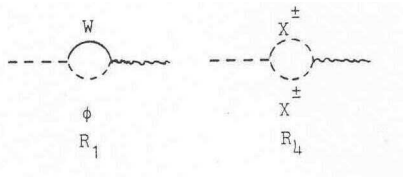

γ vertex:

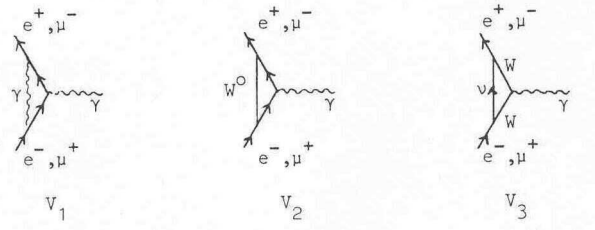

W^o vertex:

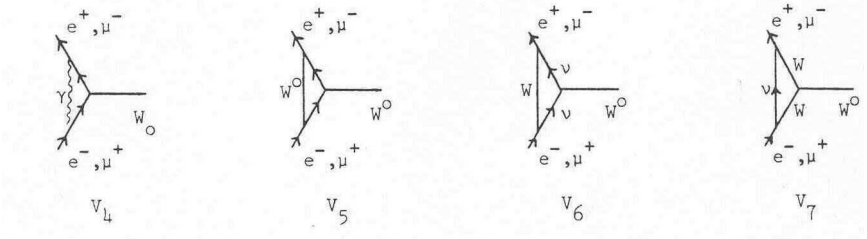

direct box:

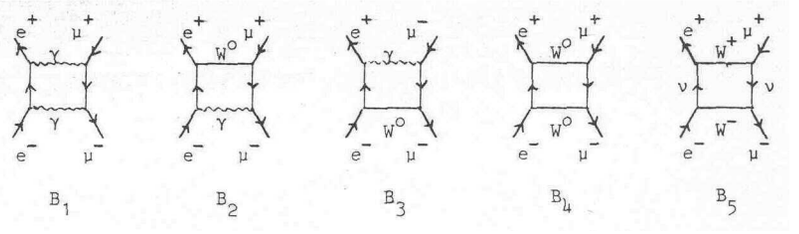

crossed box:

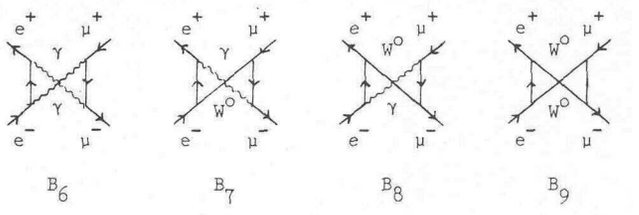

Appendix D

Two-point form factors

Our notations and conventions are those of ref. [3], except that we have factorized a factor $i\pi^2$. Thus our *A(m)* equals *A(m)* of ref. [3] divided by $i\pi^2$:

$$A(m) = \frac{1}{i\pi^2}\int \mathrm{d}^n q \frac{1}{q^2+m^2}$$

$$= m^2(-\Delta - 1 + \ln m^2), \qquad \Delta = -\frac{2}{n-4} + \gamma - \ln \pi$$

$$\gamma = \text{Eulers constant}. \tag{D.1}$$

The same holds for the *B, C* and *D* functions.

The two-point integrals occurring are

$$B_0; B_\mu; B_{\mu\nu}(p, m_1, m_2) = \frac{1}{i\pi^2}\int \mathrm{d}^n q \frac{1; q_\mu; q_\mu q_\nu}{(q^2+m_1^2)((q+p)^2+m_2^2)}. \tag{D.2}$$

The function B_μ must be proprotional to p_μ:

$$B_\mu(p, m_1, m_2) = p_\mu B_1(p, m_1, m_2). \tag{D.3}$$

This defines the function B_1. Similarly:

$$B_{\mu\nu} = p_\mu p_\nu B_{21} + \delta_{\mu\nu} B_{22}. \tag{D.4}$$

The functions B_1, B_{21} and B_{22} are algebraically related to A and B_0. These relations are obtained by multiplying eq. (D.2) with p_μ etc., and substituting

$$(qp) = \tfrac{1}{2}[(q+p)^2 + m_2^2 - (q^2 + m_1^2) - p^2 - m_2^2 + m_1^2]. \tag{D.5}$$

We **so** obtain

$$p^2 B_1 = \tfrac{1}{2}[A(m_1) - A(m_2) - (p^2 + m_2^2 - m_1^2)B_0]. \tag{D.6}$$

In case m_1 and/or m_2 are very large the expression on the right-hand side of eq. (D.6) suffers very strong cancellations: the total is very much smaller than the individual terms. For this reason we have not used these algebraic relations, except to rewrite self-energy diagrams as much as possible in a form most suitable for numerical evaluation. Further identities that we exploited are:

$$p^2 B_{21} + B_{22} = \tfrac{1}{2}\{A(m_2) + (m_1^2 - m_2^2 - p^2)B_1\},$$
$$A(m_2) - m_1^2 B_0 = p^2 B_{21} + 4B_{22} + \tfrac{1}{2}(m_1^2 + m_2^2 + \tfrac{1}{3}p^2).$$

We will now give the equations actually used to compute the various functions *B:*

$$B_0 = \Delta - \left[\ln(-p^2 - i\epsilon) + \sum_j \{\ln(1 - x_j) + F(1, x_j)\}\right],$$
$$B_1 = -\tfrac{1}{2}\Delta + \tfrac{1}{2}\left[\ln(-p^2 - i\epsilon) + \sum_j \{\ln(1 - x_j) + F(2, x_i)\}\right]. \tag{D.9}$$

The x_i are the roots of the equation $-p^2 x^2 + (p^2 + m_2^2 - m_1^2)x + m_1^2 = 0$. The function $F(n, y)$ is defined by

$$F(n, x) = -x^n \ln\frac{x-1}{x} - x^{n-1} - \tfrac{1}{2}x^{n-2} - \tfrac{1}{3}x^{n-3} \ldots - \frac{1}{n} \tag{D.10}$$

$$= \frac{1}{n+1}\frac{1}{x} + \frac{1}{n+2}\frac{1}{x^2} + \ldots, \tag{D.11}$$

$$F(n, x) = \frac{1}{x}\left\{\frac{1}{n+1} + F(n+1, x)\right\}, \tag{D.12}$$

$$\int_0^1 \mathrm{d}x\, x^n \ln(x - x_1) = \frac{1}{n+1}\{\ln(1 - x_1) + F(n+1, x_1)\}. \tag{D.13}$$

This function is rather difficult to evaluate numerically if x is large, which is evident from the form of the two equations given above. In practice we used the formula involving the logarithm if $|x| < 4$; for $|x| > 4$ we used the series development with as many terms as necessary to obtain a 12 digit precession. The cancellations, for large x, inherent in the first equation for F are the same as occurring in eqs. (D.6)-(D.8)

for large masses. Here this can be cured in the way indicated; in case of the 3- and 4-point function things are much more complicated.

$$B_{21} = \tfrac{1}{3}\Delta - \tfrac{1}{3}[\ln(-p^2 - i\epsilon) + \sum\{\ln(1-x_j) - F(3, x_j)\}] \tag{D.14}$$

$$\begin{aligned} B_{22} = \tfrac{1}{4}\Big[& -(m_1^2 + m_2^2 + \tfrac{1}{3}p^2)(\Delta + \tfrac{1}{2}) - m_2^2 + m_2^2 \ln m_2^2 \\ & + (\tfrac{1}{3}p^2 + m_1^2)\ln(-p^2 - i\epsilon) \\ & + \sum_j \{m_1^2(1-x_j)\ln(1-x_j) + m_1^2 x_j \ln(-x_j) - m_1^2 \\ & + \tfrac{1}{3}p^2(\ln(1-x_j) + F(3, x_j))\}\Big]. \end{aligned} \tag{D.15}$$

The necessary derivative B's are:

$$\frac{\partial B_0}{\partial p^2} = \frac{-1}{p^2(x_1 - x_2)}\{(1-x_1)F(1, x_1) - (1-x_2)F(2, x_2)\}, \tag{D.16}$$

$$\frac{\partial B_1}{\partial p^2} = \frac{1}{p^2(x_1 - x_2)}\{(1-x_1)F(2, x_1) - (1-x_2)F(2, x_2)\}. \tag{D.17}$$

Appendix E

Three-point form factors

As noted in appendix D we use the same conventions as in ref. [3], apart from a factor $i\pi^2$. The relevant integrals are:

$$\begin{aligned} & C_0; C_\mu; C_{\mu\nu}; C_{\mu\nu\alpha}(p_1, p_2, m_1, m_2, m_3) \\ & \quad = \frac{1}{i\pi^2}\int \mathrm{d}^n q \frac{1; q_\mu; q_\mu q_\nu; q_\mu q_\nu q_\alpha}{(q^2 + m_1^2)((q+p_1)^2 + m_2^2)((q+p_1+p_2)^2 + m_3^2)}, \end{aligned} \tag{E.I}$$

and we will often use $p_5 \equiv p_1 + p_2$. The various C may be written in terms of form-factors. The definitions are (we write p and k instead of p_1 and p_2):

$$C_\mu = p_\mu C_{11} + k_\mu C_{12}, \tag{E.2}$$

$$C_{\mu\nu} = p_\mu p_\nu C_{21} + k_\mu k_\nu C_{22} + \{pk\}_{\mu\nu} C_{23} + \delta_{\mu\nu} C_{24}, \tag{E.3}$$

$$\begin{aligned} C_{\mu\nu\alpha} = & \, p_\mu p_\nu p_\alpha C_{31} + k_\mu k_\nu k_\alpha C_{32} + \{kpp\}_{\mu\nu\alpha} C_{33}, \\ & + \{pkk\}_{\mu\nu\alpha} C_{34} + \{p\delta\}_{\mu\nu\alpha} C_{35} + \{k\delta\}_{\mu\nu\alpha} C_{36}, \end{aligned} \tag{E.4}$$

$$\{pk\}_{\mu\nu} = p_\mu k_\nu + k_\mu p_\nu, \tag{E.5}$$

$$\{kpp\}_{\mu\nu\alpha} = k_\mu p_\nu p_\alpha + p_\mu k_\nu p_\alpha + p_\mu p_\nu k_\alpha, \tag{E.6}$$

$$\{p\delta\}_{\mu\nu\alpha} = p_\mu \delta_{\nu\alpha} + p_\nu \delta_{\mu\alpha} + p_\alpha \delta_{\mu\nu}. \tag{E.7}$$

The various functions C are algebraically related to the *A*, *B*, C_0 functions. To write these down explicitly some abreviating notations are necessary. If from eq. (E.1) one of the factors in the denominator is omitted then we have a two point function. Such two point functions will be denoted by indicating the remaining masses. Thus B_{22} (2,3) is defined as the B_{22} coefficient of the integral

$$\frac{1}{i\pi^2}\int \mathrm{d}^n q \frac{q_\mu q_\nu}{(q^2+m_2^2)((q+p_2)^2+m_3^2)}.$$

Note that in the denominator we have shifted q with respect to q occurring in eq. (E.1). Next we define (remember $p_5 = p_1 + p_2$):

$$f_1 = m_1^2 - m_2^2 - p_1^2, \qquad f_2 = m_2^2 - m_3^2 - p_5^2 + p_1^2,$$
$$R_1 = \tfrac{1}{2}\{f_1 C_0 + B_0(1,3) - B_0(2,3)\},$$
$$R_2 = \tfrac{1}{2}\{f_2 C_0 + B_0(1,2) - B_0(1,3)\}.$$

The matrix X is given by

$$X = \begin{pmatrix} p_1^2 & (p_1p_2) \\ (p_1p_2) & p_2^2 \end{pmatrix}.$$

Then $(C_{11}, C_{12}) = X^{-1}(R_1, R_2)$, which stands for

$$\begin{pmatrix} C_{11} \\ C_{12} \end{pmatrix} = X^{-1}\begin{pmatrix} R_1 \\ R_2 \end{pmatrix}.$$

Further,

$$C_{24} = \tfrac{1}{4} - \tfrac{1}{2}m_1^2 C_0 + \tfrac{1}{4}(B_0(2,3) - f_1 C_{11} - f_2 C_{12}),$$
$$R_3 = \tfrac{1}{2}\{f_1 C_{11} + B_1(1,3) + B_0(2,3)\} - C_{24},$$
$$R_4 = \tfrac{1}{2}\{f_1 C_{12} + B_1(1,3) - B_1(2,3)\},$$
$$R_5 = \tfrac{1}{2}\{f_2 C_{11} + B_1(1,2) - B_1(1,3)\},$$
$$R_6 = \tfrac{1}{2}\{f_2 C_{12} - B_1(1,3)\} - C_{24},$$
$$(C_{21}, C_{23}) = X^{-1}(R_3, R_5),$$
$$(C_{22}, C_{23}) = X^{-1}(R_4, R_6).$$

The reader may note that we have more equations than unknowns, i.e., C_{23} is computed in two different ways. This provides for excellent checks on the internal consistency of the scheme.

Finally the C_3 form factors. Even if they do not occur in the particular process of this paper they can in general occur in a renormalizable theory and for completeness we list them also. Define

$$R_{11} = \tfrac{1}{2}\{f_1 C_{24} + B_{22}(1,3) - B_{22}(2,3)\},$$

$$R_{15} = \tfrac{1}{2}\{f_2 C_{24} + B_{22}(1,2) - B_{22}(1,3)\},$$
$$(C_{35}, C_{36}) = X^{-1}(R_{11}, R_{15}),$$
$$R_8 = \tfrac{1}{2}\{f_1 C_{21} + B_{21}(1,3) - B_0(2,3)\} - 2C_{35},$$
$$R_9 = \tfrac{1}{2}\{f_1 C_{22} + B_{21}(1,3) - B_{21}(2,3)\},$$
$$R_{10} = \tfrac{1}{2}\{f_1 C_{23} + B_{21}(1,3) + B_1(2,3)\} - C_{36},$$
$$R_{12} = \tfrac{1}{2}\{f_2 C_{21} + B_{21}(1,2) - B_{21}(1,3)\},$$
$$R_{13} = \tfrac{1}{2}\{f_2 C_{22} - B_{21}(1,3)\} - 2C_{36},$$
$$R_{14} = \tfrac{1}{2}\{f_2 C_{23} - B_{21}(1,3)\} - C_{35},$$
$$(C_{33}, C_{34}) = X^{-1}(R_{10}, R_{14}),$$
$$(C_{31}, C_{33}) = X^{-1}(R_8, R_{12}),$$
$$(C_{34}, C_{32}) = X^{-1}(R_9, R_{13}).$$

The above equations are again not very suitable for numerical evaluation if one or more of the masses are very large. Within the context of the calculations in this paper this is usually not very relevant, because for low energies diagrams with large masses contribute very little. The exception are diagrams that contain infinities; and inaccuracies in the functions C may then lead to inaccuracies in the renormalization procedure. We found it necessary to use approximations in the following cases:

(i) Momenta p_1^2, p_2^2 and $p_5^2 = (p_1+p_2)^2 = -s$, $m_1 = m^2$, $m_2 = M_0^2$, $m_3 = m^2$ where m is small (electron or muon mass) and M_0 large (W° mass). For $s < 0.01\, M_0^2$ we used the following approximations. Define:

$$y_1 = \tfrac{1}{2}(p_1^2 - p_2^2 + p_5^2), \qquad y_1' = y_1 - p_1^2,$$
$$y_2 = 1/(M_0^2 + p_1^2 - m^2).$$

Then,

$$C_{11} = y_2[B_1(1,3) + B_0(2,3) - 2y_2\{(p_1^2 + (p_1p_2))B_{21}(1,3) + B_{22}(1,3) - B_{22}(2,3) + (p_1p_2)B_{11}(2,3) - p_1^2 B_0(2,3)\}],$$
$$C_{12} = y_2[B_1(1,3) - B_1(2,3) - 2y_2\{(p_1^2 + (p_1p_2))B_{21}(1,3) - (p_1p_2)B_{21}(2,3) + p_1^2 B_{11}(2,3)\}].$$

Further,

$$y_3 = y_2 M_0^2\{-A(M_0) + \tfrac{5}{6}M_0^2\},$$
$$y_4 = -\tfrac{1}{6}\{A(M_0) - m^2 B_1(2,3) - \tfrac{1}{3}(M_0^2 + \tfrac{1}{2}m^2)\},$$
$$C_{21} = y_2[B_{21}(1,3) - B_0(2,3) - 4y_2\{B_{22}(2,3) + \tfrac{1}{12}y_3\}],$$

$$C_{22} = y_2\{B_{21}(1,3) - B_{21}(2,3)\},$$
$$C_{23} = y_2[B_{21}(1,3) + B_1(2,3) - 2y_2\{y_4 + B_{22}(2,3)\}],$$
$$C_{24} = y_2[B_{22}(1,3) - B_{22}(2,3) - 2y_2\{y_1' y_4 + y_1 B_{22}(2,3) + \tfrac{1}{12}p_1^2 y_3\}].$$

(ii) Momenta p_1^2, p_2^2 and $p_5^2 = (p_1+p_2)^2 = -s$, $m_1^2 = M^2$, $m_2^2 = 0$, $m_3^2 = M^2$ where M is large (charged vector boson mass). The zero mass m_2. refers to a neutrino. For $s < 0.01M^2$ we used the following approximations

$$C_{11} = -3/4M^2, \qquad C_{12} = -1/4M^2,$$
$$C_{21} = 11/18M^2, \qquad C_{22} = 1/9M^2, \qquad C_{23} = 7/36M^2,$$
$$C_{24} = \tfrac{1}{4}\Delta + \tfrac{1}{8} - \tfrac{1}{4}\ln M^2 - (3p_1^2 + 3p_2^2 + 2p_5^2)/72M^2.$$

We now consider the vertex diagrams more specifically. Many of the features which characterize the cross section contribution of these diagrams can be understood if we perform some algbraic manipulations on them. We start from the analysis of the $e^+e^-\gamma$ vertex in QED. Consider the expression

$$\Gamma^\mu_{\mathrm{QED}} = ig^3 s_\theta^3 \int d^n q \bar{v}(p_1) \frac{\gamma^\rho(-i\not{q} + m_e)\gamma^\mu[-i(\not{q}+\not{p}_5) + m_e]\gamma^\rho}{(q^2+m_e^2)((q+p_1)^2+\lambda^2)((q+p_5)^2+m_e^2)} u(p_2)$$
$$= i\pi^2 g^3 s_\theta^3 \hat{\Gamma}^\mu,$$
$$\hat{\Gamma}^\mu = -4\bar{v}(p_1)\gamma^\mu[(n-4)+1]C_{24}u(p_2)$$
$$+2\bar{v}(p_1)\gamma^\beta\gamma^\mu\gamma^\alpha u(p_2)[(C_{11}+C_{23})p_{1\alpha}p_{1\beta} + (C_{12}+C_{22})p_{2\alpha}p_{2\beta}$$
$$+(C_{11}+C_{23})p_{1\alpha}p_{2\beta} + (C_{12}+C_{23})p_{2\alpha}p_{1\beta}]$$
$$-4im_e\bar{v}(p_1)u(p_2)[(C_0+2C_{11})p_{1\mu} + (C_0+2C_{12})p_{2\mu}] - 2m_e^2\bar{v}(p_1)\gamma^\mu u(p_2)C_0, \tag{E.8}$$

and the C must be computed with

$$p_1^2 = -m_e^2, \qquad p_2^2 = -m_e^2, \qquad p_5^2 = -s,$$
$$m_1 = m_e, \qquad m_2 = \lambda, \qquad m_3 = m_e.$$

When weak interactions are also included the result depends on the A/V ratio's for the vertices as described by fig. 16.

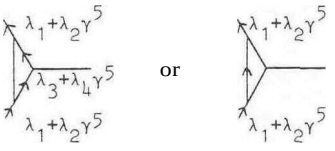

Fig. 16. A/V ratio's.

For these diagrams we can obtain the final result using

$$p_1^2 = -m_e^2, \quad p_2^2 = -m_e^2, \quad p_5^2 = -s,$$
$$m_1 = m_e, \quad m_2 = m_\nu, \quad m_3 = m_e,$$

where $m_\nu = \lambda$ or M_0, and $m_1 = m_3 = 0$, $m_2 = M$.

Referring to eq. (7.1) of sect. 7 we deduce from eq. (E.8):

$$F_\nu = \frac{g^2}{16\pi^2} k f_\nu V,$$
$$G_A = \frac{g^2}{16\pi^2} k g_A V, \tag{E.9}$$

with

$$V = -4(1+n-4)C_{24} + 2(C_{11} + C_{23})s, \tag{E.10}$$

and k is a coefficient coming from the internal vertices. Further $f_\nu = (\lambda_1^2 + \lambda_2^2)\lambda_3 + 2\lambda_1\lambda_2\lambda_4$ and $g_A = (\lambda_1^2 + \lambda_2^2)\lambda_4 + 2\lambda_1\lambda_2\lambda_3$, where we have neglected terms proportional to the lepton mass.

We conclude from eq. (E.10) that in the cross section for the first type of diagrams only C_{11}, C_{23} and C_{24} survive and the coefficient of C_{24} is $-2/s$ times the coefficient of $C_{11} + C_{23}$.

For the second type of diagrams we have

$$p_1^2 = -m_e^2, \quad p_2^2 = -m_e^2, \quad p_5^2 = -s,$$
$$m_1 = M, \quad m_2 = 0, \quad m_3 = M,$$

and for F_ν and G_A we still find an equation of the form (E.9), but now

$$V = 4(3+n-4)C_{24} - 2(C_0 + C_{11} + C_{23})s, \tag{E.11}$$

while $f_\nu = \lambda_1^2 + \lambda_2^2$ and $g_A = 2\lambda_1\lambda_2$. Eq. (E.11) implies that in the cross section for the second type of diagrams only C_0, C_{11}, C_{23}, C_{24} appear and the coefficient of C_{24} is $-6/s$ times the coefficient of $C_0 + C_{11} + C_{23}$. The pole part of C_{24} is easily computed and gives $+\frac{1}{4}\Delta$; eq. (E.10) reads now

$$V = -4(C_{24} - \tfrac{1}{2}) + 2(C_{11} + C_{23})s,$$

and eq. (E.11)

$$V = 12(C_{24} - \tfrac{1}{6}) - 2(C_0 + C_{11} + C_{23})s.$$

Appendix F

The four-point form factors

As noted in appendix D we use the same convention as in ref. [2], apart from a factor $i\pi^2$. The one-loop integrals occurring in renormalizable theories are:

$$D_0; D_\mu; D_{\mu\nu}; D_{\mu\nu\alpha}; D_{\mu\nu\alpha\beta} = \frac{1}{i\pi^2} \times \int d_n q \frac{1; q_\mu; q_\mu q_\nu; q_\mu q_\nu q_\alpha; q_\mu q_\nu q_\alpha q_\beta}{(q^2+m_1^2)((q+p_1)^2+m_2^2)((q+p_1+p_2)^2+m_3^2)((q+p_1+p_2+p_3)^2+m_4^2)}. \tag{F.1}$$

As a matter of notation we introduce $p_5 = p_1 + p_2$ and $p_6 = p_2 + p_3$. The form factors are then functions of $p_1^2 \ldots p_6^2$ and $m_1^2 \ldots m_4^2$. Again, as in appendix E, we use a condensed notation for two- and three-point functions obtained from eq. (F.1) by omitting two or one factor in the denominator (and possibly shifted q in that denominator). Thus $C_{24}(2,3,4)$ denotes the form factor C_{24} of the expression

$$\frac{1}{i\pi^2} \int d_n q \frac{q_\mu q_\nu}{(q^2+m_2^2)((q+p_2)^2+m_3^2)((q+p_2+p_3)^2+m_4^2)}.$$

The various D are now defined by (we use p, k and l instead of p_1 p_2 and p_3)

$$D_\mu = p_\mu D_{11} + k_\mu D_{12} + l_\mu D_{13}, \tag{(F.2)}$$

$$D_{\mu\nu} = p_\mu p_\nu D_{21} + k_\mu k_\nu D_{22} + l_\mu l_\nu D_{23} + \{pk\}_{\mu\nu} D_{24} + \{pl\}_{\mu\nu} D_{25} + \{kl\}_{\mu\nu} D_{26} + \delta_{\mu\nu} D_{27}. \tag{F.3}$$

We refer to eqs. (E.5)-(E.7) for the notations used. In the equations below we also drop the indices μ, ν etc.,

$$\begin{aligned} D_{\mu\nu\alpha} = {} & ppp D_{31} + kkk D_{32} + lll D_{33} + \{kpp\} D_{34} \\ & + \{lpp\} D_{35} + \{pkk\} D_{36} + \{pll\} D_{37} + \{lkk\} D_{38} \\ & + \{kll\} D_{39} + \{pkl\} D_{310} + \{p\delta\} D_{311} + \{k\delta\} D_{312} + \{l\delta\} D_{313}, \end{aligned} \tag{F.4}$$

$$\begin{aligned} D_{\mu\nu\alpha\beta} = {} & pppp D_{41} + kkkk D_{42} + llll D_{43} + \{ppPk\} D_{44} \\ & + \{pppl\} D_{45} + \{kkkp\} D_{46} + \{kkkl\} D_{47} + \{lllp\} D_{48} \\ & + \{lllk\} D_{49} + \{ppkk\} D_{410} + \{ppll\} D_{411} + \{kkll\} D_{412} \\ & + \{ppkl\} D_{413} + \{kkpl\} D_{414} + \{llpk\} D_{415} + \{pp\delta\} D_{416} \\ & + \{kk\delta\} D_{417} + \{ll\delta\} D_{418} + \{pk\delta\} D_{419} + \{pl\delta\} D_{420} \\ & + \{kl\delta\} D_{421} + \{\delta\delta\} D_{422}. \end{aligned} \tag{F.5}$$

The notations used are straight generalities of those given before, eqs. (E.5)-(E.7). For example

$$\{ppkl\}_{\mu\nu\alpha\beta} = p_\mu p_\nu \{kl\}_{\alpha\beta} + p_\mu p_\alpha \{kl\}_{\nu\beta} + p_\mu p_\beta \{kl\}_{\nu\alpha} + p_\nu p_\alpha \{hl\}_{\mu\beta} + p_\nu p_\beta \{kl\}_{\mu\alpha} + p_\alpha p_\beta \{kl\}_\mu ,$$

$$\{\delta\delta\}_{\mu\nu\alpha\beta} = \delta_{\mu\nu}\delta_{\alpha\beta} + \delta_{\mu\alpha}\delta_{\nu\beta} + \delta_{\mu\beta}\delta_{\nu\alpha} .$$

The matrix X is now (we use again p_1, p_2 and

$$X = \begin{pmatrix} P_1^2 & (p_1p_2) & (p_1p_3) \\ (p_1p_2) & p_2^2 & (p_2p_3) \\ (p_1p_3) & (p_2p_3) & p_3^2 \end{pmatrix}.$$

Further,

$$f_1 = m_1^2 - m_2^2 - p_1^2 ,$$

$$f_2 = m_2^2 - m_3^2 + p_1^2 - p_5^2 ,$$

$$f_3 = m_3^2 - m_4^2 - p_4^2 + p_5^2 ,$$

$$R_{20} = \tfrac{1}{2}\{f_1 D_0 + C_0(1,3,4) - C_0(2,3,4)\} ,$$

$$R_{21} = \tfrac{1}{2}\{f_2 D_0 + C_0(1,2,4) - C_0(1,3,4)\} ,$$

$$R_{22} = \tfrac{1}{2}\{f_3 D_0 + C_0(1,2,3) - C_0(1,2,4)\} ,$$

$$(D_{11}, D_{12}, D_{13}) = X^{-1}(R_{20}, R_{21}, R_{22}) ,$$

$$D_{27} = -m_1^2 D_0 - \tfrac{1}{2}\{f_1 D_{11} + f_2 D_{12} + f_3 D_{13} - C_0(2,3,4)\} ,$$

$$R_{30} = \tfrac{1}{2}\{f_1 D_{11} + C_{11}(1,3,4) + C_0(2,3,4)\} - D_{27} ,$$

$$R_{33} = \tfrac{1}{2}\{f_1 D_{12} + C_{11}(1,3,4) - C_{11}(2,3,4)\} ,$$

$$R_{36} = \tfrac{1}{2}\{f_1 D_{13} + C_{12}(1,3,4) - C_{12}(2,3,4)\} ,$$

$$R_{31} = \tfrac{1}{2}\{f_2 D_{11} + C_{11}(1,2,4) - C_{11}(1,3,4)\} ,$$

$$R_{34} = \tfrac{1}{2}\{f_2 D_{12} + C_{12}(1,2,4) - C_{11}(1,3,4)\} - D_{27} ,$$

$$R_{37} = \tfrac{1}{2}\{f_2 D_{13} + C_{12}(1,2,4) - C_{12}(1,3,4)\} ,$$

$$R_{32} = \tfrac{1}{2}\{f_3 D_{11} + C_{11}(1,2,3) - C_{11}(1,2,4)\} ,$$

$$R_{35} = \tfrac{1}{2}\{f_3 D_{12} + C_{12}(1,2,3) - C_{12}(1,2,4)\} ,$$

$$R_{38} = \tfrac{1}{2}\{f_3 D_{13} - C_{12}(1,2,4)\} - D_{27} ,$$

$$R_{39} = -m_1^2 D_0 + C_0(2,3,4) ,$$

$$(D_{21}, D_{24}, D_{25}) = X^{-1}(R_{30}, R_{31}, R_{32}) ,$$

$$(D_{24}, D_{22}, D_{26}) = X^{-1}(R_{33}, R_{34}, R_{35}) ,$$

$$(D_{25}, D_{26}, D_{23}) = X^{-1}(R_{36}, R_{37}, R_{38}),$$

$$D_{311} = -\tfrac{1}{2}m_1^2 D_{11} - \tfrac{1}{4}\{f_1 D_{21} + f_2 D_{24} + f_3 D_{25} + C_0(2,3,4)\},$$

$$D_{312} = -\tfrac{1}{2}m_1^2 D_{12} - \tfrac{1}{4}\{f_1 D_{24} + f_2 D_{22} + f_3 D_{26} - C_{11}(2,3,4)\},$$

$$D_{313} = -\tfrac{1}{2}m_1^2 D_{13} - \tfrac{1}{4}\{f_1 D_{25} + f_2 D_{26} + f_3 D_{23} - C_{12}(2,3,4)\},$$

$$R_{41} = \tfrac{1}{2}\{f_1 D_{21} - C_0(2,3,4) + C_{21}(1,3,4)\} - 2D_{311},$$

$$R_{42} = \tfrac{1}{2}\{f_2 D_{21} - C_{21}(1,3,4) + C_{21}(1,2,4)\},$$

$$R_{43} = \tfrac{1}{2}\{f_3 D_{21} - C_{21}(1,2,4) + C_{21}(1,2,3)\},$$

$$R_{44} = \tfrac{1}{2}\{f_1 D_{24} + C_{21}(1,3,4) + C_{11}(2,3,4)\} - D_{312},$$

$$R_{50} = \tfrac{1}{2}\{f_1 D_{22} - C_{21}(2,3,4) + C_{21}(1,3,4)\},$$

$$R_{56} = \tfrac{1}{2}\{f_1 D_{23} - C_{22}(2,3,4) + C_{22}(1,3,4)\},$$

$$R_{45} = \tfrac{1}{2}\{f_2 D_{24} - C_{21}(1,3,4) + C_{23}(1,2,4)\} - D_{311},$$

$$R_{51} = \tfrac{1}{2}\{f_2 D_{22} - C_{21}(1,3,4) + C_{22}(1,2,4)\} - 2D_{312},$$

$$R_{57} = \tfrac{1}{2}\{f_2 D_{23} - C_{22}(1,3,4) + C_{22}(1,2,4)\},$$

$$R_{46} = \tfrac{1}{2}\{f_3 D_{24} - C_{23}(1,2,4) + C_{23}(1,2,3)\},$$

$$R_{52} = \tfrac{1}{2}\{f_3 D_{22} - C_{22}(1,2,4) + C_{22}(1,2,3)\},$$

$$R_{58} = \tfrac{1}{2}\{f_3 D_{23} - C_{22}(1,2,4)\} - 2D_{313},$$

$$(D_{31}, D_{34}, D_{35}) = X^{-1}(R_{40}, R_{41}, R_{42}),$$

$$(D_{36}, D_{32}, D_{38}) = X^{-1}(R_{50}, R_{51}, R_{52}),$$

$$(D_{37}, D_{39}, D_{33}) = X^{-1}(R_{56}, R_{57}, R_{58}),$$

$$(D_{34}, D_{36}, D_{310}) = X^{-1}(R_{44}, R_{45}, R_{46}),$$

$$D_{416} = \tfrac{1}{3}[-m_1^2 D_{21} + \tfrac{1}{2}\{C_0(2,3,4) - f_1 D_{31} - f_2 D_{34} - f_3 D_{35}\}],$$

$$D_{417} = \tfrac{1}{3}[-m_1^2 D_{22} + \tfrac{1}{2}\{C_{21}(2,3,4) - f_1 D_{36} - f_2 D_{32} - f_3 D_{38}\}],$$

$$D_{418} = \tfrac{1}{3}[-m_1^2 D_{23} + \tfrac{1}{2}\{C_{22}(2,3,4) - f_1 D_{37} - f_2 D_{39} - f_3 D_{33}\}],$$

$$D_{419} = \tfrac{1}{3}[-m_1^2 D_{24} - \tfrac{1}{2}\{C_{11}(2,3,4) + f_1 D_{34} + f_2 D_{36} + f_3 D_{310}\}],$$

$$D_{420} = \tfrac{1}{3}[-m_1^2 D_{25} - \tfrac{1}{2}\{C_{12}(2,3,4) + f_1 D_{35} + f_2 D_{310} + f_3 D_{37}\}],$$

$$D_{421} = \tfrac{1}{3}[-m_1^2 D_{26} + \tfrac{1}{2}\{C_{23}(2,3,4) - f_1 D_{310} - f_2 D_{38} - f_3 D_{39}\}],$$

$$D_{422} = \tfrac{1}{6}[-m_1^2 D_{27} + C_{24}(2,3,4) + \tfrac{1}{12} - p_1^2 D_{416} - p_2^2 D_{417} - p_3^2 D_{418}$$
$$- \lambda(p_1 p_2) D_{419} - \lambda(p_1 p_3) D_{420} - \lambda(p_2 p_3) D_{421}],$$

$$R_{60} = \tfrac{1}{2}\{f_1 D_{32} - C_{31}(2,3,4) + C_{31}(1,3,4)\},$$

$$R_{61} = \tfrac{1}{2}\{f_2 D_{32} - C_{31}(1,3,4) + C_{32}(1,2,4)\} - 3D_{41}$$
$$R_{62} = \tfrac{1}{2}\{f_3 D_{32} - C_{32}(1,2,4) + C_{32}(1,2,3)\},$$
$$R_{63} = \tfrac{1}{2}\{f_1 D_{31} + C_0(2,3,4) + C_{31}(1,3,4)\} - 3D_{41}$$
$$R_{64} = \tfrac{1}{2}\{f_2 D_{31} - C_{31}(1,3,4) + C_{31}(1,2,4)\},$$
$$R_{65} = \tfrac{1}{2}\{f_3 D_{31} - C_{31}(1,2,4) + C_{31}(1,2,3)\},$$
$$R_{66} = \tfrac{1}{2}\{f_1 D_{33} - C_{32}(2,3,4) + C_{32}(1,3,4)\},$$
$$R_{67} = \tfrac{1}{2}\{f_2 D_{33} - C_{32}(1,3,4) + C_{32}(1,2,4)\},$$
$$R_{68} = \tfrac{1}{2}\{f_3 D_{33} - C_{32}(1,2,4)\} - 3D_{418},$$
$$R_{69} = \tfrac{1}{2}\{f_1 D_{37} + C_{22}(2,3,4) + C_{34}(1,3,4)\} - D_{418}$$
$$R_{70} = \tfrac{1}{2}\{f_2 D_{37} - C_{34}(1,3,4) + C_{34}(1,2,4)\},$$
$$R_{71} = \tfrac{1}{2}\{f_3 D_{37} - C_{34}(1,2,4)\} - 2D_{420},$$
$$R_{72} = \tfrac{1}{2}\{f_1 D_{34} - C_{11}(2,3,4) + C_{31}(1,3,4)\} - 2D_{41}$$
$$R_{73} = \tfrac{1}{2}\{f_2 D_{34} - C_{31}(1,3,4) + C_{33}(1,2,4)\} - D_{416}$$
$$R_{74} = \tfrac{1}{2}\{f_3 D_{34} - C_{33}(1,2,4) + C_{33}(1,2,3)\},$$
$$R_{75} = \tfrac{1}{2}\{f_1 D_{38} - C_{33}(2,3,4) + C_{33}(1,3,4)\},$$
$$R_{76} = \tfrac{1}{2}\{f_2 D_{38} - C_{33}(1,3,4) + C_{32}(1,2,4)\} - 2D_{42}$$
$$R_{77} = \tfrac{1}{2}\{f_3 D_{38} - C_{32}(1,2,4)\} - D_{417},$$
$$(D_{46}, D_{42}, D_{47}) = X^{-1}(R_{60}, R_{61}, R_{62}),$$
$$(D_{41}, D_{44}, D_{45}) = X^{-1}(R_{63}, R_{64}, R_{65}),$$
$$(D_{48}, D_{49}, D_{43}) = X^{-1}(R_{66}, R_{67}, R_{68}),$$
$$(D_{411}, D_{415}, D_{48}) = X^{-1}(R_{69}, R_{70}, R_{71}),$$
$$(D_{44}, D_{410}, D_{413}) = X^{-1}(R_{72}, R_{73}, R_{74}),$$
$$(D_{414}, D_{47}, D_{412}) = X^{-1}(R_{75}, R_{76}, R_{77}).$$

All equations of appendices D, E and F have been programmed, and specifying $p_1^2 \ldots p_6^2$ and $m_1^2 \ldots m_4^2$ the program returns the complex values of all quantities $B_0 - D_{422}$*. The computing time taken on a CDC6500 is of the order of 1 second [7]. If none of the masses are large with respect to all external momenta then there is no problem with accuracy. If some of the masses are large then the results become rapidly inaccurate, with the higher order form factors deteriorating first.

* This program returns the values according to the conventions of ref. [3]. Thus the form-factors occurring in this paper obtain after division by $i\pi^2$.

The overdetermination of the form factors can be used to obtain information on this. In the calculation reported in this paper only the difficulties signalled in appendix E needed attention; after that results were accurate over a range of 1 to 200 GeV, with photon masses as low as a few keV. To achieve this it was however necessarh to compute accurately (13 digits) the arguments of the Spence functions occurring in the equations for C_0 and D_0 of ref. [3]; in intermediate stages this required computation accurate up to more than 40 decimal digits.

References

[1] G. 't Hooft, Nucl. Phys. B35 (1971) 167.
[2] P. Van Nieuwenhuizen, Nucl. Phys. B28 (1977) 381;
F. Berends, R. Gaemers and R. Gastmans, Nucl. Phys. B57 (1973) 381, B67 (1974) 541.
[3] G. 't Hooft and M. Veltman, Nucl. Phys. B153 (1979) 365.
[4] F. Berends, R. Gaemers and R. Gastmans, Nucl. Phys. B63 (1973) 381.
[5] H. Strubbe, Comp. Phys. Comm. 8 (1974) 1.
[6] F. Berends and R. Gastmans *in* Electromagnetic interactions of hadrons, ed. A. Donnachie and G. Shaw (Plenum, London).
[7] M. Veltman, FORMF, a CDC program for the computation of one-loop form factors.